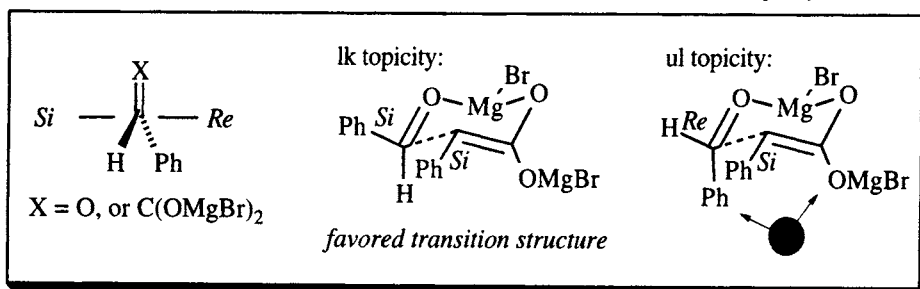
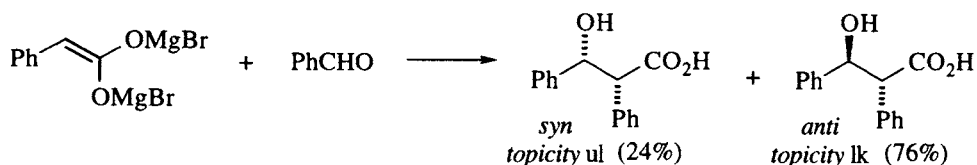


Aldol and Michael Additions of Allyls and Enolates

In this chapter, the discussion of additions to carbonyls continues with the aldol addition reaction and the mechanistically similar allyl addition reactions, both examples of “ π -transfer” additions illustrated in Figure 4.1. Also discussed are asymmetric Michael addition reactions.

The aldol condensation is one of the oldest reactions in organic chemistry, dating back to the first half of the 19th century, but about 1980 it underwent a renaissance after methods were developed to stop the reaction at the stage of the initial addition product, with a high degree of stereoselectivity. Much of the excitement and interest in asymmetric synthesis since that time has been due to the development of highly selective aldol addition reactions and the mechanistically similar allyl addition reactions. We begin the chapter with the latter, because the allyl addition is irreversible and because the transition state assemblies are somewhat less complex than those of the aldol additions.

Scheme 5.1 illustrates the transition structure most often invoked to explain the selectivities observed in π -transfer 1,2-carbonyl additions (*cf.* Figure 4.1): the so-called Zimmerman-Traxler transition structure [1]. This model, which was originally proposed to rationalize the selectivity of the Ivanov reaction, has its shortcomings (as will be seen) and suffers from an oversimplification when applied to enolates, in that it illustrates a monomeric enolate (*cf.* section 3.1 and ref. [2-4]). Nevertheless, it serves the very useful purpose of providing a simple means to rationalize relative and absolute configurations in almost all of the asymmetric 1,2-additions we will see. The favored transition structure has *lk* topology (*Si/Si*



Scheme 5.1. The Zimmerman-Traxler transition state model for the Ivanov reaction [1].

illustrated) because the alternative has a pseudo 1,3-diaxial interaction between the aldehyde phenyl and the magnesium alkoxide. Because the magnesium alkoxide is on a trigonal carbon in the 6-membered ring, this repulsive interaction is not large, and the selectivity for the anti product is only 76% [1].¹

5.1 1,2-Additions of allyl metals and metalloids

Most allylic organometallic or organometalloid systems are reactive enough to add to aldehyde carbonyls without the aid of additional Lewis acids, the notable exception being allyl silanes (reviews: [7-15]). Often, the allylic metal or metalloid atom itself activates the carbonyl, and a highly organized six-membered ring transition structure similar to the Zimmerman-Traxler model results. This section deals with cases where chiral ligands on the metal or on an acid catalyst induce selectivity by interligand asymmetric induction. Reactions of allyl metal compounds in which the metal-bearing carbon is stereogenic are not covered.

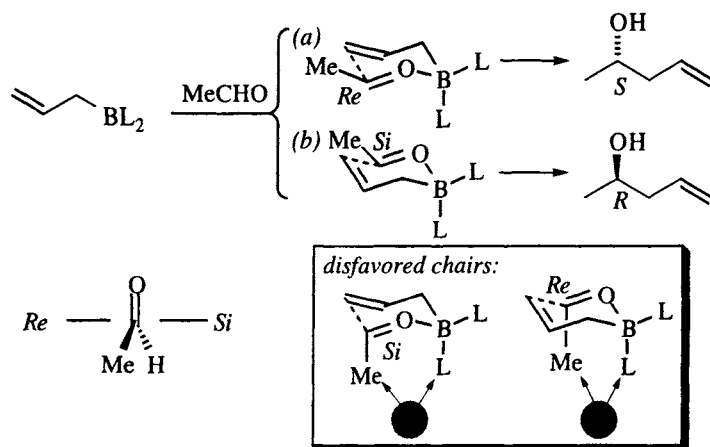
In order to explain the chemistry of allylic metals, the reactions of allylic boron compounds [8,12-14] are covered in detail. The boron chemistry is divided into four parts: simple enantioselectivity (addition of $\text{CH}_2=\text{CHCH}_2-$, creating one new stereocenter), simple diastereoselectivity of crotyl additions (relative configuration after $\text{CH}_3\text{CH}=\text{CHCH}_2-$ addition, where neither reagent is chiral), single asymmetric induction with chiral allyl boron compounds (one and two new stereocenters), and double asymmetric induction (both reactants chiral, one and two new stereocenters). Then follows a brief discussion of other allyl metal systems.

5.1.1 Simple enantioselectivity

Scheme 5.2 illustrates the enantiomeric chair transition structures and products for the addition of an allyl borane to acetaldehyde. Note that in assembly *a*, the *Re* face of the aldehyde is attacked, producing the *S* alcohol. Conversely, attack on the *Si* face of the aldehyde produces the *R* alcohol (assembly *b*). In the inset are shown two alternative chair transition structures, which originate by reversing the position of the aldehyde methyl and hydrogen substituents of assemblies *a* and *b* (or equivalently, by flipping the chair). These are destabilized by severe 1,3-diaxial interactions between the aldehyde methyl and one of the ligands on boron. Note that the boron ligand is fully axial (unlike the pseudoaxial magnesium alkoxide in Scheme 5.1), and the boron-oxygen bond is fairly short.² These two differences mean that the repulsive interaction is quite strong, and the aldehyde is preferentially oriented with its nonhydrogen substituent equatorially. Thus the simple concepts of conformational analysis of substituted cyclohexanes, applied to the Zimmerman-Traxler model, provide a basis for a “first approximation” analysis of these closed (cyclic) transition structures.

¹ We will use the *syn/anti* nomenclature [5] to describe the relative configuration of aldol stereoisomers, and the *lk/ul* nomenclature [6] to describe the topology of the reaction. For definitions, see glossary, Section 1.6.

² A B–O bond is 1.36–1.47 Å, whereas a Mg–O bond is 2.0–2.1 Å [16].



Scheme 5.2. Cyclic transition states for allyl boron additions.

Unless there is a chiral ligand on boron, assemblies *a* and *b* of Scheme 5.2 are enantiomeric and the product will be racemic. If the ligand is chiral, then the transition structures are diastereomeric and the products will be formed in unequal amounts under conditions of kinetic control (Chapter 1). Figure 5.1 illustrates several chiral boron reagents that have been tested in the allyl boration reaction, with typical enantioselectivities for each.

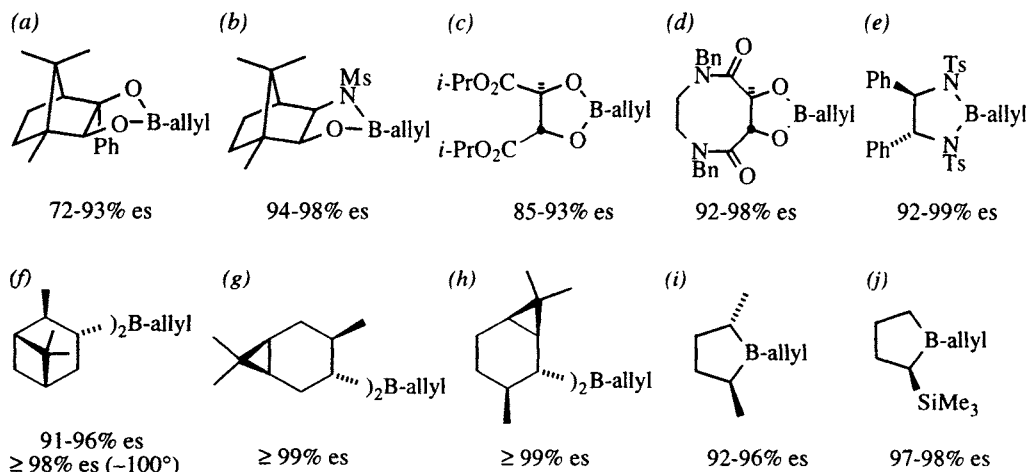


Figure 5.1. Chiral boron compounds for asymmetric allyl addition to achiral primary, secondary, and tertiary alkyl, vinyl, and aryl aldehydes, and their typical enantioselectivities (*a-e* at -78° , *g-j* at -100°). (*a*) [17]; (*b*) [18]; (*c*) [19]; (*d*) [19]; (*e*) [20]; (*f-h*) [21-24]; (*i-j*) [25].

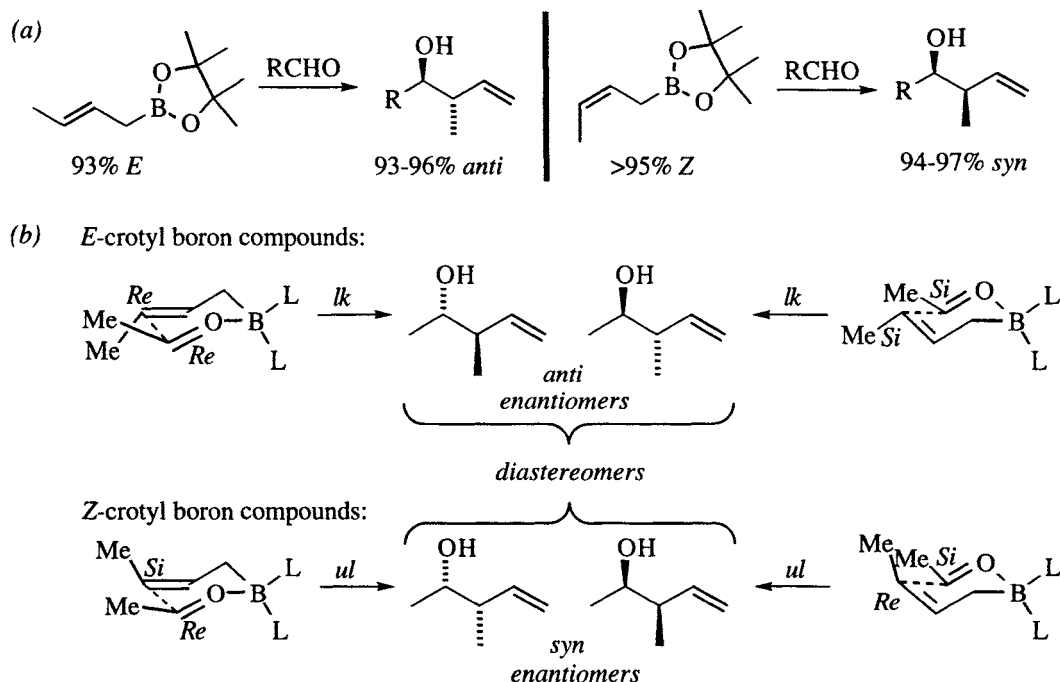
5.1.2 Simple diastereoselectivity

When there is a substituent on the allyl double bond, geometric isomers are possible and two new stereocenters are formed. The transition structures in Scheme 5.3 illustrate how the *E*-crotyl boron compound affords racemic anti addition product and the *Z*-crotyl compound affords the syn product.³ For the *E* isomer, the

³ This assumes that there are no isomerizations that precede the addition. For discussions of such phenomena for boranes and boronates, see ref. [26].

most stable chair presents the *Re* face of the aldehyde to the *Re* face of the double bond, or vice versa (*lk* topicity). These two transition structures are enantiomeric (and therefore isoenergetic in the absence of a chiral influence), as are the anti products. Likewise, the *Z*-crotyl species assembles with *ul* topicity, presenting the *Re* face of the aldehyde to the *Si* face of the double bond, or vice versa, which produces the syn addition product.

Note that reversing the face of only one component of the assembly reverses the topicity and the relative configuration of the stereocenters in the product. For example, exchanging the positions of the methyl and hydrogen in either the aldehyde or the crotyl moiety of the *lk* transition structure changes the topicity to *ul*, and the syn product would be produced. As before (Scheme 5.2) exchanging the aldehyde substituents causes severe 1,3-interactions with the axial boron ligand. Therefore, the tendency is for *lk* topicity for *E*-crotyl species, giving anti products and *ul* topicity for *Z*-crotyl compounds, giving syn products.

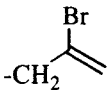
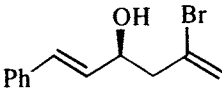
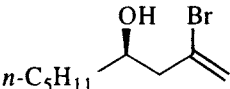
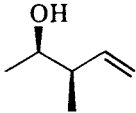
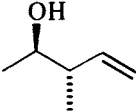
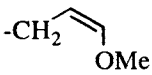
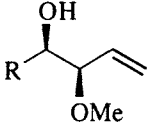
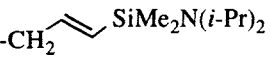
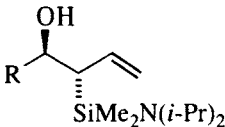


Scheme 5.3. (a) Stereospecificity (within experimental error) of crotyl borane additions to aldehydes, R = Me, Et, *i*-Pr, Ph [26]. (b) Transition structures for stereospecific addition of crotyl boron compounds to aldehydes.

5.1.3 Single asymmetric induction

Figure 5.1 lists a number of auxiliaries for asymmetric allyl addition to aldehydes. Substituted allyl boron compounds have also been used in reactions with achiral aldehydes. Table 5.1 lists several examples of 2- and 3-substituted allyl boron compounds, and the products derived from their addition. Note that for the *E*- and *Z*-crotyl compounds, the enantioselectivity indicated is for the isomer illustrated. In some cases, there was more than one of the other three possible isomers found as well.

Table 5.1. Asymmetric addition of substituted allyl boron compounds to aldehydes. Ligands are illustrated in Figure 5.1.

Entry	RCHO	L ₂ BR	Product	% Yield	% es	Ref
1	<i>E</i> - cinnamyl	 L ₂ = <i>ent</i> -5.1e		79	94	[20]
2	<i>n</i> - C ₅ H ₁₁ -	"		77	>99	[20]
3	CH ₃ -	<i>Z</i> -crotyl L ₂ =5.1f		75	95	[27]
4	CH ₃ -	<i>E</i> -crotyl L ₂ =5.1f		78	95	[27]
5	CH ₃ -	 L ₂ =5.1f	 (R = CH ₃)	59	95	[28]
6	Ph-	"	" (R = Ph)	75	95	[28]
7	<i>n</i> - C ₆ H ₁₃ -	 L ₂ =5.1f	 (R = <i>n</i> -C ₆ H ₁₃)	52	>95	[29]
8	<i>c</i> -C ₆ H ₁₁ -	"	" (R = <i>c</i> -C ₆ H ₁₁)	63	>95	[29]
9	Ph-	"	" (R = Ph)	50	>95	[29]

5.1.4 Double asymmetric induction

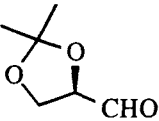
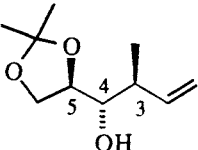
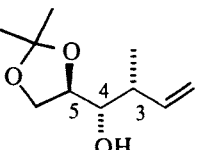
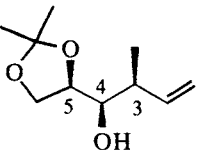
When the boron ligands and the aldehyde are both chiral, the inherent stereoselectivities of each partner may be either matched or mismatched (Chapter 1). In principle, a chiral aldehyde could derive facial selectivity from either the Felkin-Anh-Heathcock model (Figures 4.8 and 4.10) or the Cram-chelate model (Figure 4.11). However, because the boron of these reagents can accept only one additional ligand, chelation is not possible. Therefore only the Felkin-Anh-Heathcock effects

are operative in these reactions, and they are usually relatively weak, with diastereoselectivities of $\leq 70\%$. The high diastereoselectivities of many of the auxiliaries illustrated in Figure 5.1 can therefore be used to control the relative and absolute configuration of both of the new stereocenters in the addition product. Table 5.2 lists selected examples of double asymmetric induction with two α -alkoxyaldehydes and several auxiliaries (the 4,5-anti isomer is favored by Cram's rule).

Table 5.2. Double asymmetric induction in addition of allyl boron compounds to aldehydes. Ligands are illustrated in Figure 5.1.

Entry	RCHO	L ₂ BR	Product	% Yield	% ds	Ref
1		allyl L ₂ =5.1e		80	96	[20]
2		allyl L ₂ =5.1e		—	98	[20]
3		allyl L ₂ =5.1a		87	96	[30]
4	"	allyl L ₂ =5.1c	"	85	93	[19,31]
5	"	allyl L ₂ =5.1d	"	84	98	[19]
6	"	allyl L ₂ = ent-5.1c		90	98	[31]
7	"	allyl L ₂ = ent-5.1d	"	81	99.7	[19,31]
8	"	<i>E</i> -crotyl L ₂ =5.1c		85	96	[8,32,33]
9	"	<i>E</i> -crotyl L ₂ =5.1i	"	74	86	[25]

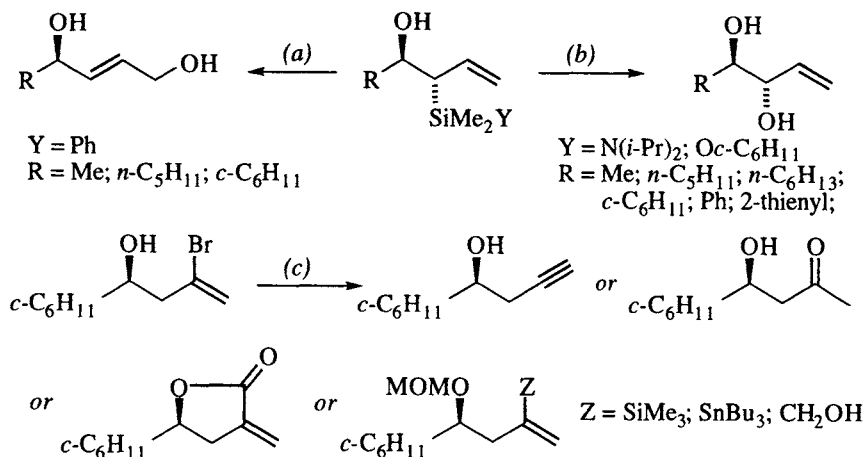
Table 5.2 (cont.). Double asymmetric induction in addition of allyl boron compounds. Ligands are illustrated in Figure 5.1.

Entry	RCHO	L ₂ BR	Product	% Yield	% ds	Ref
10		<i>E</i> -crotyl L ₂ =5.1a		85	72	[30]
11	"	<i>E</i> -crotyl L ₂ = <i>ent</i> -5.1c	"	87	87	[8,32,33]
12	"	<i>E</i> -crotyl L ₂ = <i>ent</i> -5.1i	"	71	96	[25]
13	"	<i>Z</i> -crotyl L ₂ =5.1a		86	>98	[30]
14	"	<i>Z</i> -crotyl L ₂ =5.1c	"	90	76	[8,33]
15	"	<i>Z</i> -crotyl L ₂ = <i>ent</i> -5.1c	"	84	>99	[8,33]
16	"	<i>Z</i> -crotyl L ₂ = <i>ent</i> -5.1i	"	66	92	[34]
17	"	<i>Z</i> -crotyl L ₂ =5.1i		65	82	[34]

Noteworthy among these examples is the ability to achieve high diastereoselectivity for both the 3,4-syn and 3,4-anti isomers, almost independent of the chirality sense of the aldehyde. Comparison of several examples show the expected trends for matched and mismatched pairs (*cf.* entry pairs 1/2, 4/6, 5/7, 9/12, 16/17). Note that either 3,4-anti diastereomer can be obtained with 96% ds (entries 8 and 12); the two 3,4-syn isomers are also available selectively (entries 13-16 and 17), although only one ligand (5.1i) is selective for the 3,4-syn-4,5-syn product (entry 17) that is a mismatched pair (*cf.* entry 16). Note that with Roush's tartrate ligand (Figure 5.1c), the *E*-crotyl mismatched pair is more selective than the matched pair (entries 8/11; for a rationale, see ref. [33]), and the matched and mismatched pair give the same major product isomer with the *Z*-crotyl compound (entries 14/15).

Several substituted allyl and crotyl derivatives have been designed to increase the usefulness of the boron-mediated allyl addition of aldehydes. For example, silanes such as those shown in Table 5.1, entries 7-9, can be stereospecifically converted to

hydroxyls [29,35] or transformed into alcohols with a formal 1,3-hydroxy migration [36]. Additionally, vinyl bromides such as those shown in Table 5.1, entries 1 and 2 can be converted into a number of functional groups by standard chemical means [20]. Examples of these transformations are shown in Scheme 5.4. Note also that ozonolysis of any of these adducts give “aldol” adducts (Section 5.2).



Scheme 5.4. Transformations of functionalized addition products. (a) [36]; (b) [29,35]; (c) [20].

5.1.5 Other allyl metals

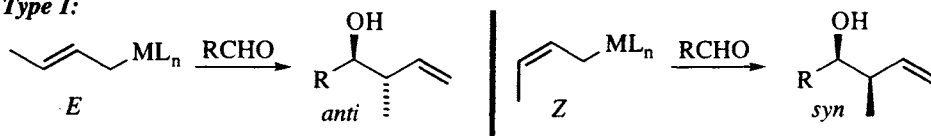
In addition to boron, a number of other metals have been used in π -transfer addition reactions (reviews: [7-11,14,15]. Based on stereochemical tendencies and mechanistic considerations, these reagents have been classified into three groups, as illustrated in Scheme 5.5 [8,37]:

- Type 1.** Reagents that are stereospecific in the sense that an *E*-crotyl isomer affords the anti addition product (*lk* topicity) and a *Z*-crotyl isomer affords the syn product (*ul* topicity). The transition structure is thought to be a closed chair, analogous to the Zimmerman-Traxler transition structure (Scheme 5.1).
- Type 2.** Reactions that are catalyzed by Lewis acids and are stereoconvergent to syn adducts for either the *E*- or the *Z*-crotyl organometallics (*ul* topicity). The transition structure is usually considered to be open (acyclic), but the exact nature of the transition state is still a matter of discussion [8,9].
- Type 3.** Allyl organometallics that are (usually) generated *in situ* and which equilibrate to the more stable *E*-crotyl species, then add via a closed, Zimmerman-Traxler transition structure producing anti adducts preferentially [8].

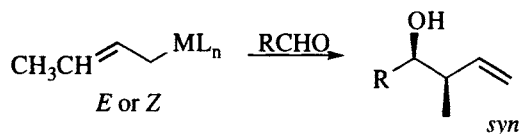
The boron-containing compounds discussed in the previous sections are typical of Type 1 reagents. Also included in this group are reactions of allyl aluminums and uncatalyzed reactions of allyl tin reagents [8,37].

Reactions that fit Type 2 are catalyzed by Lewis acids which coordinate to the carbonyl oxygen of the aldehyde, thereby precluding coordination by the allyl metal. Such reactions proceed *via* an open transition state. As indicated previously, allyl silanes are not reactive enough to add to aldehydes without acid catalysis, so

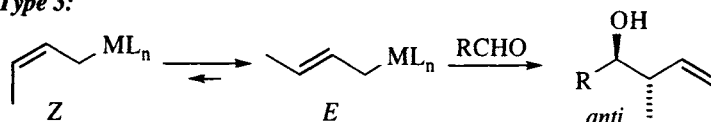
Type 1:



Type 2:

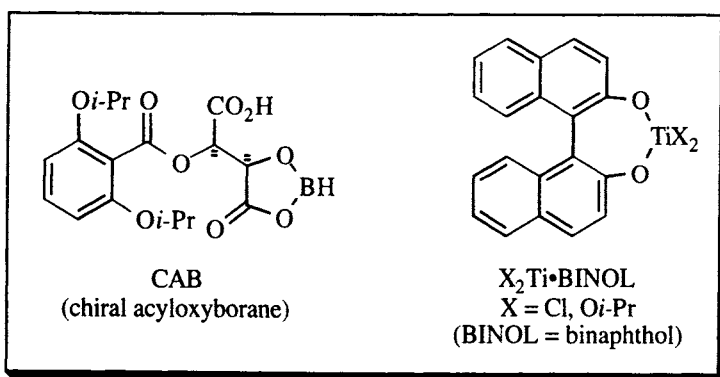
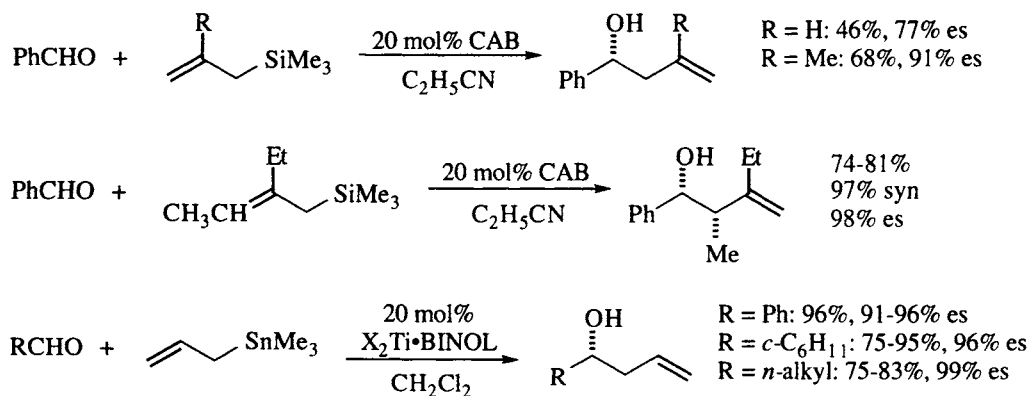


Type 3:



Scheme 5.5. Mechanistic types for allyl addition to carbonyls. Types 1 and 3 proceed through transition structures similar to those in Scheme 5.3 [8,37].

they fall into this category [37]. Allyl stannane additions may be catalyzed by Lewis acids, so stannanes sometimes fall into this group [38,39], as do allyl titanium reagents [8,9,37]. Scheme 5.6 shows some enantioselective examples of allylsilane



Scheme 5.6. Enantioselective additions of allyl silanes [40] and allyl stannanes [41,42], mediated by chiral catalysts.

additions [40] and allyl stannane [41,42] additions; many enantioselective additions of allylstannanes involve chirality transfer from the stannane where the allylic carbon bearing the tin is stereogenic [9,15], and are not discussed herein.

Figure 5.2 illustrates the six possible open transition structures for the Lewis acid mediated addition of allyl metals to an aldehyde. Note that for each topicity, there are two synclinal arrangements and one antiperiplanar. Several factors must be considered in explaining the observed *ul* topicity of these reactions (giving syn relative configuration in the products), and a number of rationales have been offered. If one assumes that the conformation is antiperiplanar in the transition state, then structure *a* would be favored over *d*, since this arrangement minimizes the interaction between in the aldehyde substituent, R, and the methyl of the crotyl group.

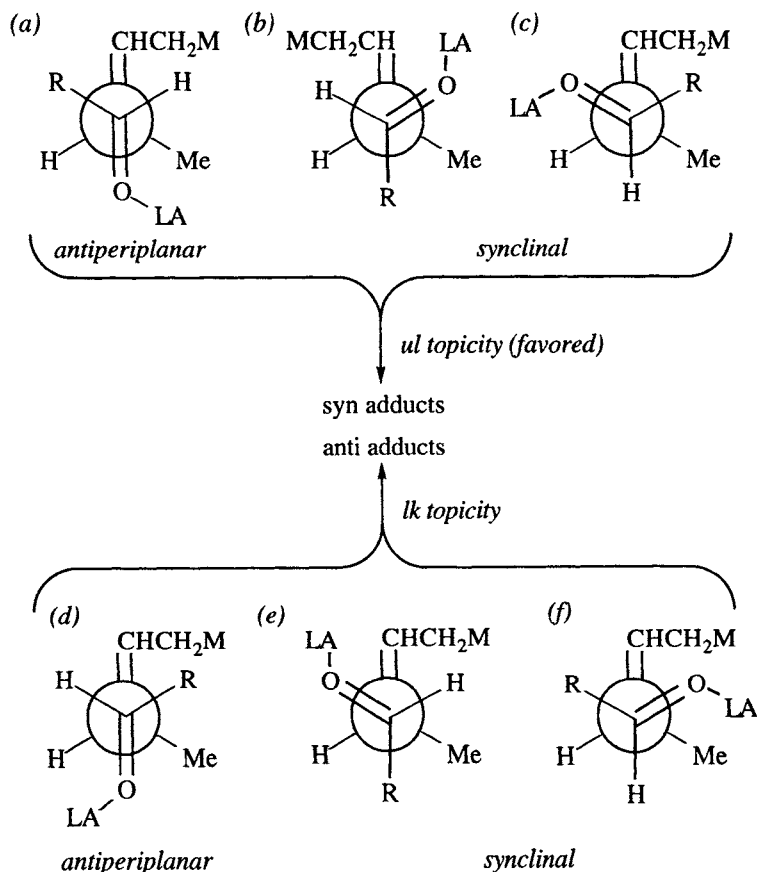


Figure 5.2. Newman projections of possible open transition structures for Lewis acid (LA) catalyzed additions to aldehydes.

On the other hand, Seebach suggested in 1981 that the topicity of a number of reactions (including these) may be explained by having the double bonds oriented in a synclinal arrangement.⁴ He reasoned that steric repulsion between the R and

⁴ For a discussion of the Seebach rule as applied to the Michael reaction, see Figure 5.9 and the accompanying discussion.

CHCH₂M moieties would favor *b* over *c* and *e* over *f*. Then, assuming that the nucleophile approaches the carbonyl along the Bürgi-Dunitz trajectory (Section 4.1.3), either the hydrogen (in *b*) or the methyl group (in *e*) must be squeezed in between the alkyl group and hydrogen of the aldehyde. The former would be favored. This hypothesis was offered as a “topological rule” (not a mechanism).

Later, studies of intramolecular silane [37] and stannane [39] additions offered a direct comparison between synclinal arrangement *c* and antiperiplanar arrangement *d*. The former is favored. Because of the intramolecular nature of the addition, conformations analogous to the other possibilities were not possible.

Allyl chromium, titanium and zirconium reagents fall into the Type 3 category. Enantioselective reactions in this class are relatively rare, although the diastereoselectivities can be quite high (reviews: [7,8,15]).

5.2 Aldol additions⁵

The Ivanov reaction (Scheme 5.1) is an early example of an aldol addition reaction that proceeded selectively. There has been an enormous amount of work done in this area, and only a small amount of the developmental work will be covered here. A large number of chiral auxiliaries and catalysts have been developed, but we will concentrate on only a few, which suffice to provide an understanding of the structural factors that influence selectivity. The transition structures presented in the following discussion are oversimplifications, in that the enolate and its metal are represented as monomers, when in fact they are not [2-4]. On the other hand, much of the available data may be rationalized on the basis of these structures, so the simplification is justified in the absence of detailed structural and configurational information about mixed aggregate transition structures.

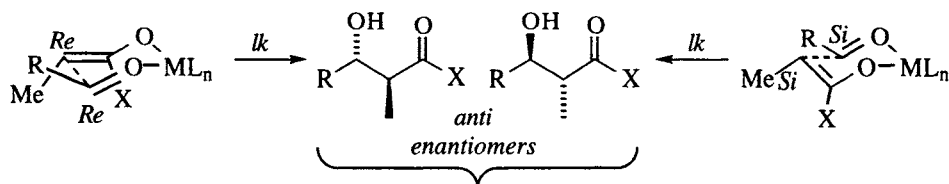
5.2.1 Simple diastereoselectivity

Kinetic control. The Zimmerman-Traxler model, as applied to propionate and ethyl ketone aldol additions, is shown in Scheme 5.7 (note the similarity to the boron-mediated allyl additions in Scheme 5.3). Based on this model, we would expect a significant dependence of stereoselectivity on the enolate geometry, which is in turn dependent on the nature of X and the deprotonating agent (see section 3.1.1). In addition, the configuration and selectivity of the kinetically controlled aldol addition is dependent on the size of the substituents on the two reactants.

Figure 5.3 illustrates both enantiomers of most of the possible transition structures that have been postulated for aldol additions of R₁CH₂COX enolates. In the closed transition structures (Figure 5.3a,b), the chair conformations would normally be expected to predominate, but in certain instances a boat may be

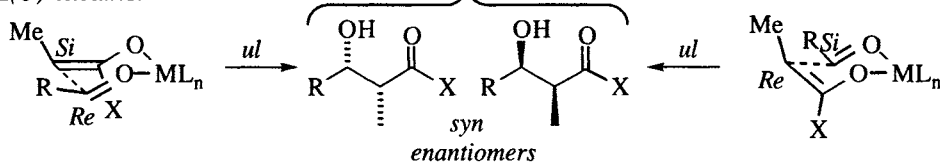
⁵ Note the distinction between the aldol *condensation*, in which α,β -unsaturated carbonyls are formed, and the aldol *addition*, which is stopped at the β -hydroxy carbonyl stage. For reviews of the early literature, mostly focusing on the aldol condensation, see ref. [43,44]. For reviews of the aldol addition, see ref. [16,45-51] (Li and Mg enolates), [52] (B and Al enolates), and [53] (transition metal enolates).

E(O)-enolates:



diastereomers

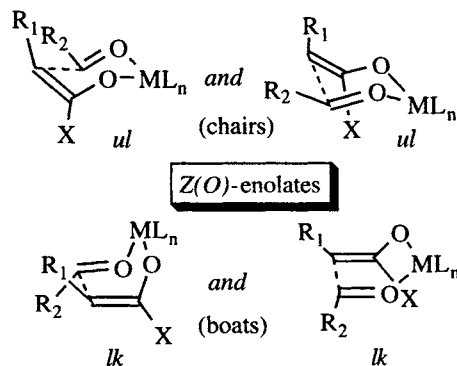
Z(O)-enolates:



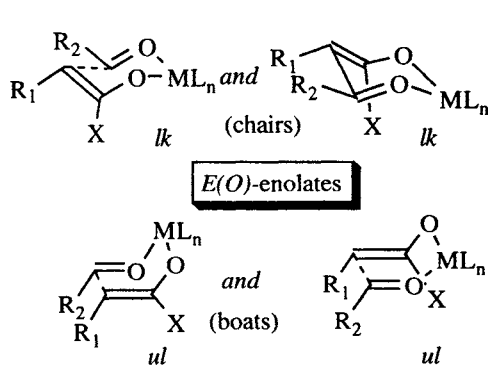
Scheme 5.7. Transition structures for stereoselective propionate additions to aldehydes.

preferable.⁶ For the open transition structures, study of the intramolecular addition of silyl ethers, catalyzed by Lewis acids, showed a moderate preference for an *anti* conformation [59]. In intermolecular cases, the choice between open structures of *ul* or *lk* topology will be governed by the relative magnitude of the gauche interactions between R_1 and either R_2 or ML_n on the aldehyde.

(a) Closed transition structures



(b) Closed transition structures



(c) Open transition structures

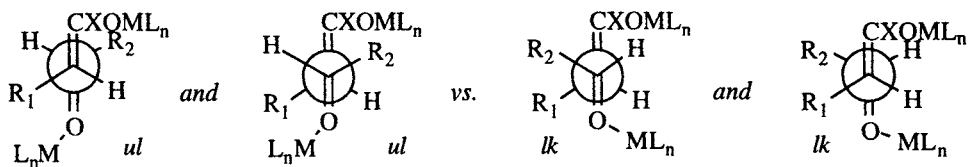
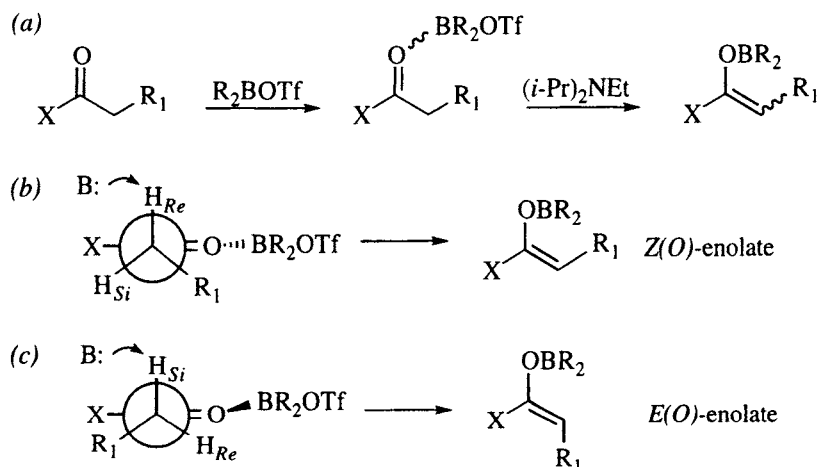


Figure 5.3. (a) Chair and boat transition structures for *Z(O)*-enolates. (b) Chair and boat transition structures for *E(O)*-enolates. (c) *ul* and *lk* open transition structures. Note that in all cases, the topology is such that *ul* → *syn*; *lk* → *anti*.

⁶ Computational studies predict that the geometry (chair, half-chair, boat, etc) depends on the nature of R_1 , R_2 , and M . Theory also predicts that *Z*-enolates prefer a closed chair, but that *E*-enolates may prefer a boat [54–56]. For an empirical rule for predicting aldol topology, see ref. [57]. For an investigation into the effect of metal and solvent on transition structures, see ref. [58].

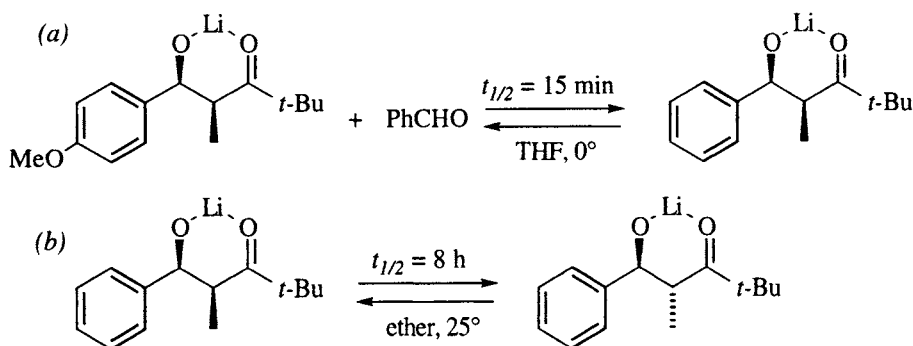
The stereoselectivity of the aldol addition often depends on the selectivity of enolate formation. Ireland's rationale for the selective formation of lithium *Z(O)*-enolates of ketones, amides, and imides, and the selective formation of ester *E(O)*-enolates was outlined in section 3.1.1 [60]. The rationale for the selective formation of *E(O)*- and *Z(O)*-boron enolates by reaction with dialkylboron triflate and a tertiary amine [61] is shown in Scheme 5.8 [52,62]. The boron triflate coordinates to the carbonyl oxygen, thereby increasing the acidity of the α -proton so that it can be removed by amine bases, as shown in Scheme 5.8a. In most cases, the stereochemical situation is as shown in Scheme 5.8b. The boron is trans to the CH_2R_1 , R_1 is antiperiplanar to X, and removal of the H_{Re} proton gives the *Z(O)*-enolate. Note that for amides ($\text{X} = \text{NR}_2$), $\text{A}^{1,3}$ strain between R_1 and NR_2 particularly destabilizes the *E(O)*-enolate. In certain instances, a repulsive van der Waals interaction between the X and BR_2OTf moieties may be particularly severe (e.g., *t*-BuS– and Bu_2BOTf), such that the boron is oriented trans to X, which forces R_1 synperiplanar to X to avoid the boron ligands, as illustrated in Scheme 5.8c. Removal of the H_{Si} proton then gives the *E(O)*-enolate.



Scheme 5.8. Rationale for the stereoselective formation of boron enolates [62]. (a) If the boron is trans to X, $\text{A}^{1,3}$ strain considerations force R_1 syn to X, and removal of the proton from a conformation in which the C–H bond is perpendicular to the carbonyl affords the *E(O)*-enolate; (b) when the boron is cis to X, R_1 may orient anti to X, and the *Z(O)*-enolate ensues.

Not all aldol additions exhibit a dependence of product configuration on enolate geometry. Acid catalyzed aldols [45], some base catalyzed aldols [58], and aldols of some transition metal enolates [63,64] show no such dependency. For example, zirconium enolates afford syn adducts (*ul* topicity) independent of enolate geometry for a number of propionates [63,64]. As shown in Scheme 5.9, two explanations have been proposed to explain the behavior of zirconium enolates. One explanation (Scheme 5.9a) is that the closed transition structure changes from a chair for the *Z(O)*-enolate to a boat for the *E(O)*-enolate [16,63,65]. Another hypothesis is that these additions occur via an open transition structure. Although the original authors [64] suggested an open transition structure, they did not provide an illustration.

To achieve kinetic control in the aldol addition reaction, it does not matter if the rate for the retro aldol is fast, as long as the relative rates for syn vs. anti addition is large. As an example, consider the following “case study”. Let us assume that the rate of *ul* addition for a *Z(O)*-enolate (to give syn adduct) is significantly faster than the rate of *lk* addition (giving anti adduct), such that $k_{syn}/k_{anti} = 100$. Under these conditions, a retro aldol must occur 100 times before one syn \rightarrow anti isomerization can occur. The actual rates of these individual processes can be measured with experiments such as those illustrated in Scheme 5.10 [68]. In Scheme 5.10a, aldehyde exchange clearly involves a retro aldol, and has a half-life of 15 minutes. In Scheme 5.10b, isomerization to the more stable anti isomer has a half-life of 8 hours at a higher temperature. Because the retro aldol and the *ul* addition are both much faster than the unfavored *lk* addition, even the crossover is syn-selective.



Scheme 5.10. (a) Aldehyde exchange and (b) syn-anti isomerization of aldolates [68].

In summary, the following generalizations have emerged for aldol additions under kinetic control:

1. *Z(O)*-enolates are highly syn-selective (*ul* topicity) when X is fairly large [51].
2. *Z(O)*-enolates with a large R_1 (such as an isopropyl or *tert*-butyl) give anti products (*lk* topicity) selectively [51].
3. *E(O)*-enolates are highly anti-selective (*lk* topicity) only with a very large X group (such as 2,6-di-*t*-butylphenol) [51].
4. For a closed transition structure, shorter M–O bond lengths amplify the van der Waals interactions between R_1 , R_2 , and X relative to enolates with longer bond lengths, resulting in higher stereoselectivities [16]. With boron enolates for example, *Z(O)*-enolates are highly syn selective [52].

5.2.2 Single asymmetric induction

For the addition of acetate and methyl ketone enolates (one new stereocenter), a number of approaches have been taken to induce enantioselectivity (review: [69]); one of these methods will be mentioned in the succeeding section, along with the propionate and ethyl ketone additions. In the open transition structures of Figure 5.3, each illustrated *lk* or *ul* pair is enantiomeric in the absence of any stereocenters in the two reactants. Introduction of a chirality element converts the paired transition structures (*i.e.*, transition structures of the same topicity) and products from enantiomers to diastereomers, and allows diastereoselection under either

kinetic or thermodynamic control. There are three opportunities for introduction of chirality: a chiral auxiliary (X^*), and the two sites of Lewis acid (ML_n^*) coordination: the enolate and the aldehyde oxygens. In principle, either one, two, or three could be chiral, allowing for the possibility of single, double, and even triple asymmetric induction.

The following discussion is organized by the 'location' of the introduced chirality: X (intraligand asymmetric induction) or ML_n (interligand asymmetric induction). Additionally, there is the possibility of a chirality center in the aldehyde, which will normally have an observable influence only in cases where the stereocenter is close to the carbonyl (*i.e.*, Cram's rule situations - see Chapter 4). Most of the examples that have been published to date include chirality centers in either X or ML_n , but not both.

Intraligand asymmetric induction. The first example of an auxiliary-based asymmetric aldol addition was reported by the Enders group, who used the enolate of a SAMP hydrazone in a crossed aldol [70]. This method afforded good yields, but only modest selectivities. Introduction of chirality in X (Figure 5.3) produces an enolate that affords much higher selectivities. Some of the more popular and effective auxiliaries are shown in Figure 5.4. The first of these (Figure 5.4a, R = methyl) was evaluated in racemic form by Heathcock in 1979, as its lithium $Z(O)$ -enolate [71,72]. Later, a synthesis of the S -enantiomer from S -*tert*-leucine (S -*tert*-butylglycine) was reported [73]. A similar auxiliary was reported by the Masamune group in 1980 (Figure 5.4b, R = methyl), which afforded outstanding selectivities as its boron $Z(O)$ -enolate. Initially [5] the racemate was resolved, but subsequently a chiron synthesis was reported using mandelic acid [74]. Both the Heathcock and the Masamune auxiliaries are self-immolative (*cf.* section 1.2, p. 2): 'removal' of the auxiliary by oxidative cleavage of the α -alkoxyketone to a carboxylic acid destroys the stereocenter. Figure 5.4c illustrates one of the most frequently used auxiliaries, the oxazolidinone imides developed in the Evans laboratory in 1981 [75]. These auxiliaries, which are made from amino alcohols such as valinol and phenylalaninol, can be cleaved to an acid, aldehyde, or an alcohol [76,77] *cf.* Scheme 3.16 and 3.17), and the auxiliary can be recovered in good yield. Reaction of either the boron $Z(O)$ -enolates [75] or the zirconium $E(O)$ - or $Z(O)$ -enolates [78] are highly

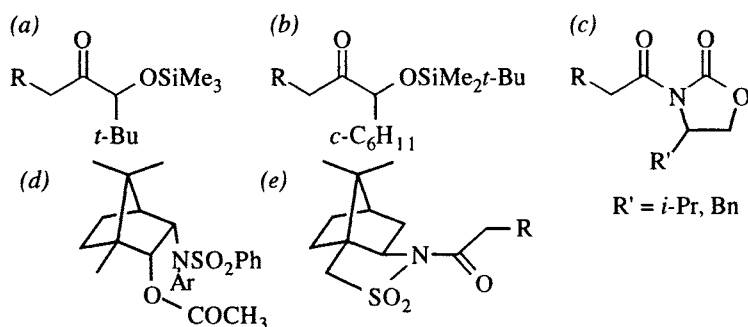


Figure 5.4. Chiral auxiliaries for asymmetric aldol additions. (a) racemic [71,72], from *tert*-leucine (*tert*-butyl glycine) [73]; (b) from mandelic acid [5,74]; (c) from valine or phenylalanine [75]; (d) from camphor [79]; (e) from camphor [80,81].

selective. None of the auxiliaries shown in Figure 5.4a-c are particularly selective when R is hydrogen (*i.e.*, 'acetate' enolates). The acetate shown in Figure 5.4d, reported by Helmchen in 1985 [79], is particularly good in this regard. A more

Note that each *E(O)*- or *Z(O)*-enolate will have a choice of two Zimmerman-Traxler transition structures. Thus (see Scheme 5.11), a *Z(O)*-enolate may add through nonchelated path a or chelated path c, both of which afford syn adducts, but of opposite absolute configuration at the two new stereocenters. Likewise, an *E(O)*-enolate may add *via* path b or d, affording diastomeric anti adducts.

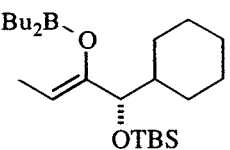
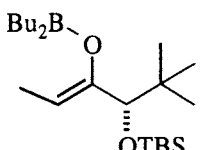
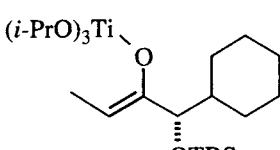
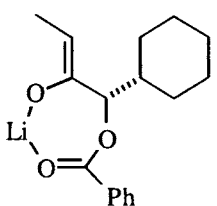
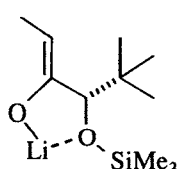
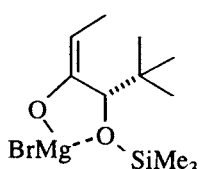
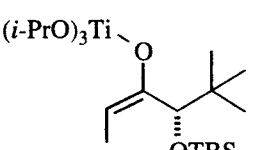
Highly selective additions of these auxiliaries have been achieved *via* all four of the postulated pathways. Table 5.3 lists several examples. For example, *Z(O)*-dibutylboron enolates (entries 1, 2) often have selectivities of >99%, and are postulated to proceed through nonchelated path a [73,74]. The reason path c cannot compete is that the boron cannot accommodate more than four ligands, and two of the ligands are non-exchangeable alkyl groups. Additionally, boron enolates are not reactive enough to add to aldehydes unless the latter are coordinated to a Lewis acid. In the absence of external acids, then, the boron of the enolate must activate the aldehyde by coordination and its two available ligand sites are occupied by the enolate and the aldehyde oxygens.

When the α -hydroxyl is silylated with a *tert*-butyldimethylsilyl group, chelation is difficult no matter what the metal. Lithium enolates of the TBS ethers are not particularly selective in their additions to aldehydes, but transmetalation to titanium affords enolates that are highly selective in their addition reactions (Table 5.3, entry 3, [84]). Acylation of the oxygen with a benzoyl group and deprotonation with LDA affords an enolate that gives the relative configuration shown in path a, although chelation by the benzoyl carbonyl oxygen is postulated (entry 4, [85]). With a smaller trimethylsilyl group, a lithium cation can simultaneously coordinate the enolate oxygen, the siloxyl oxygen, and the aldehyde oxygen. Thus, the *Z(O)*-lithium enolate affords syn adducts according to path c (entry 5, [73]).

Deprotonation of the ketone educt with *N*-(bromomagnesio)-2,2,6,6-tetramethylpiperidide affords the *E(O)*-enolate selectively. Addition of the magnesium *E(O)*-enolate having a trimethylsiloxy group affords anti adducts (entry 6, [73]), and is postulated to occur *via* chelated path d (Scheme 5.11). Transmetalation of the *tert*-butyldimethylsiloxy-protected magnesium *E(O)*-enolate affords a titanium enolate that cannot chelate, and adds to aldehydes *via* path b (entry 7, [73]). In this case, only benzaldehyde afforded selectivity lower than 95%.

A highly versatile auxiliary is the Evans oxazolidinone imide (Figure 5.4c, see also Scheme 3.16), available by condensation of amino alcohols [86,87] with diethyl carbonate [86]. Deprotonation by either LDA or dibutylboron triflate and a tertiary amine affords only the *Z(O)*-enolate. Scheme 5.12 illustrates open and closed transition structures that have been postulated for these *Z(O)*-enolates under various conditions, and Table 5.4 lists typical selectivities for the various protocols. The first to be reported (and by far the most selective) was the dibutylboron enolate (Table 5.4, entry 1), which cannot activate the aldehyde and simultaneously chelate the oxazolidinone oxygen [75]. Dipolar alignment of the auxiliary and approach of the aldehyde from the *Re* face of the enolate affords syn adduct with outstanding diastereoselection, presumably *via* the closed transition structure illustrated in Scheme 5.12a [75]. The other syn isomer can be formed under two different types of conditions. In one, a titanium enolate is postulated to chelate the oxazolidinone

Table 5.3. Asymmetric additions of the Heathcock-Masamune enolates. The "Path" column indicates the product configuration and the proposed transition structure from Scheme 5.11.

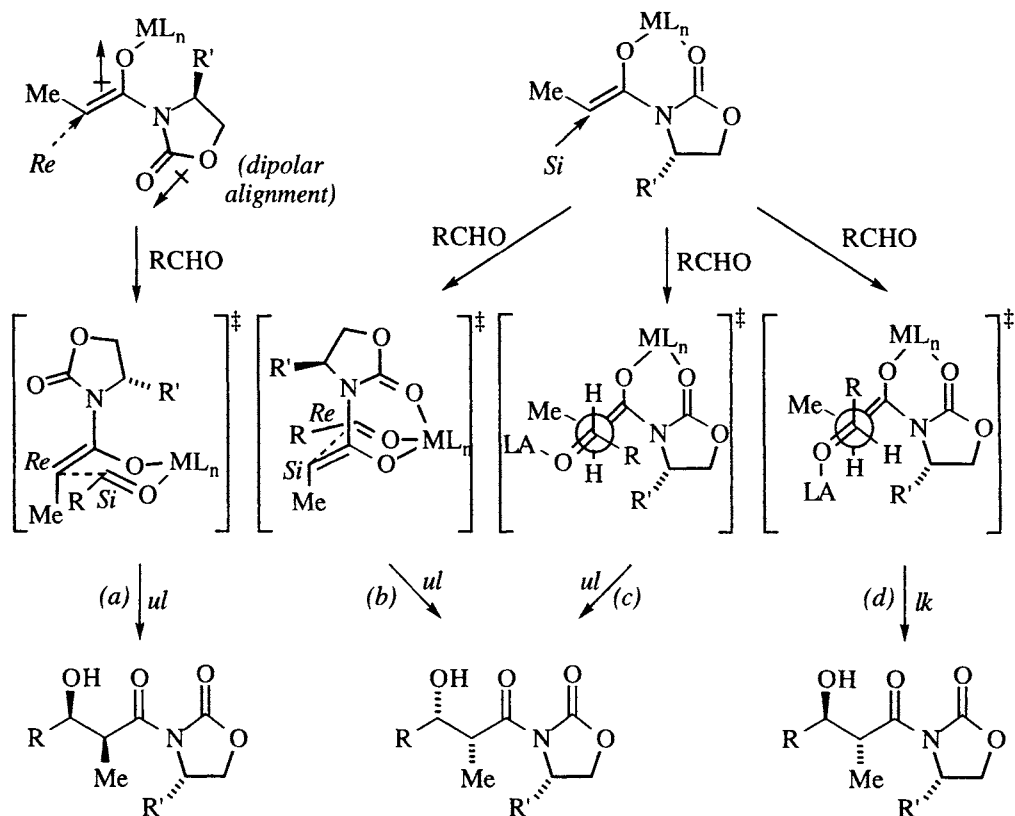
Entry	Enolate	Path	RCHO	% Yield	% ds	Ref
1		a	Et, <i>i</i> -Pr, Ph, BnO(CH ₂) ₂	70-85	≥97	[74]
2		a	<i>i</i> -Pr, <i>t</i> -Bu, Ph, BnO(CH ₂) ₂	75-80	>95	[73]
3		a	Et, <i>i</i> -Pr, <i>t</i> -Bu, Ph	75-88	≥98	[84]
4		a	Et, <i>i</i> -Pr, Ph	67-96	86-97	[85]
5		c	<i>i</i> -Pr, <i>t</i> -Bu, Ph	75-80	>95	[73]
6		d	<i>i</i> -Pr, <i>t</i> -Bu, Ph	75-85	92-95	[73]
7		b	Me, <i>i</i> -Pr, <i>t</i> -Bu, Ph	85-88	80->95	[73]

oxygen [88]⁸ or sulfur of an oxazolidinethione [89] exposing the *Si* face of the enolate (Scheme 5.12b). Additional coordination of the aldehyde and addition via

⁸ Recall that the titanium enolate of the Heathcock and Masamune auxiliaries (Table 5.3, entries 3 and 7) were postulated to occur by a *nonchelating* pathway. However, in those cases, the potential

nonchelated enolate:

chelated enolate:



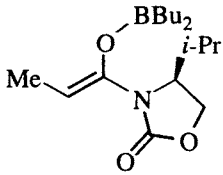
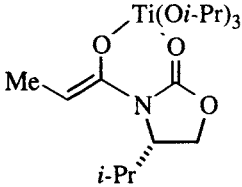
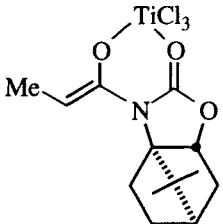
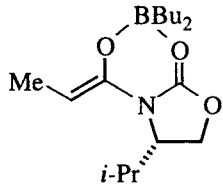
Scheme 5.12. Open and closed transition structures for aldol additions of Evans's imides.

the closed transition structure shown in Scheme 5.12b affords excellent selectivity (Table 5.4, entries 2 and 3).

If the boron enolate is allowed to react with an aldehyde in the presence of another Lewis acid (LA), the addition is thought to occur *via* the open transition structures shown in Scheme 5.12c and d [66]. If the Lewis acid is small, the preferred orientation is as shown in Scheme 5.12c, which minimizes the gauche interaction between the methyl and R groups on the forming bond (Table 5.4, entry 4). Both SnCl₄ and TiCl₄ are relatively 'small' because of the long metal - oxygen bond. If the Lewis acid is large, the interaction between the Lewis acid and the methyl may outweigh the methyl/R gauche interaction. When the aldehyde is complexed to diethylaluminum chloride, the Lewis acid is effectively larger than either the tin or titanium complexes because of the shorter Al-O bond compared to either Sn-O or Ti-O, and because the ligands on the aluminum are relatively bulky. In this instance, the other face of the aldehyde will present itself to the enolate affording the anti adduct, as shown in Scheme 5.12d (Table 5.4, entry 5).

chelating atom was a severely crowded TBS ether oxygen, as opposed to the more basic and less crowded urethane carbonyl oxygen in the Evans auxiliary.

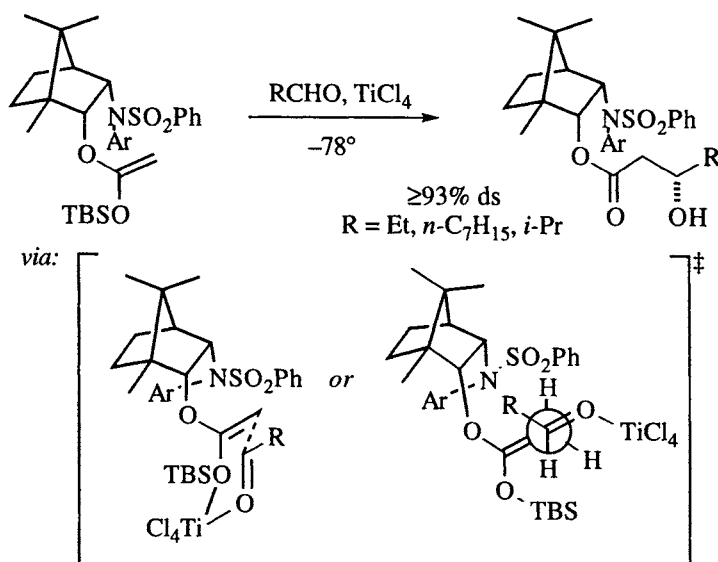
Table 5.4. Asymmetric additions of the Evans imide enolates. The "Path" column indicates the product configuration and the proposed transition structure from Scheme 5.12.

Entry	Enolate	Path	RCHO	% Yield	% ds	Ref
1		a	Bu, <i>i</i> -Pr, Ph	75-88	>99	[75]
2		b	Bu, <i>i</i> -Pr, Ph	56-75	85-92	[88]
3		b	<i>n</i> -Pr, <i>i</i> -Pr, 1-propenyl, Ph	84-88	97-99	[89]
4		c	Et, <i>i</i> -Pr, <i>i</i> -Bu, <i>t</i> -Bu, 2-propenyl, Ph (·SnCl4 or TiCl4)	50-68	87-93	[66]
5	"	d	Et, <i>i</i> -Pr, <i>i</i> -Bu, <i>t</i> -Bu, 2-propenyl, Ph (·Et2AlCl)	62-86	74-95	[66]

For syntheses requiring the syn adducts, it is more practical to use the boron enolate without additional Lewis acids [75], since the auxiliary is available as either enantiomer and is recoverable.⁹ On the other hand, the anti adducts are (so far) only available by the diethylaluminum chloride/boron enolate protocol [66]. Similar principles may be used to prepare syn and anti halohydrins by aldol addition of α -halo acetate enolates of Evans imides [90,91].

A weakness of the Heathcock Masamune and Evans auxiliaries is their inability

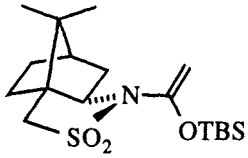
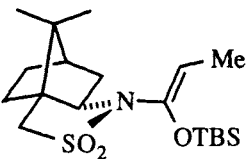
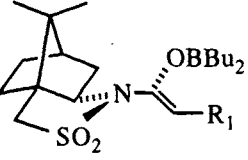
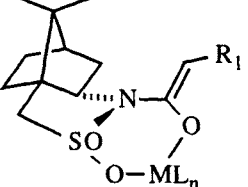
Zimmerman-Traxler transition structure, as shown on the lower left [79], however the open structure shown in the lower right, which does not require coordination of the bulky silyloxy group to titanium, should also be considered. The aldehyde may be oriented to avoid the large *tert*-butyldimethylsilyl (TBS) group as shown, with the R group away from the TBS. Both of these models have the aldehyde approaching the enol ether from the front face, opposite the side that is shielded by the sulfonamide. Note also that the siloxy group is oriented downward, to avoid the sulfonamide. An anti-selective addition (92% ds) was also reported for the reaction of the *E(O)*-enol ether of this auxiliary with isobutyraldehyde [79].



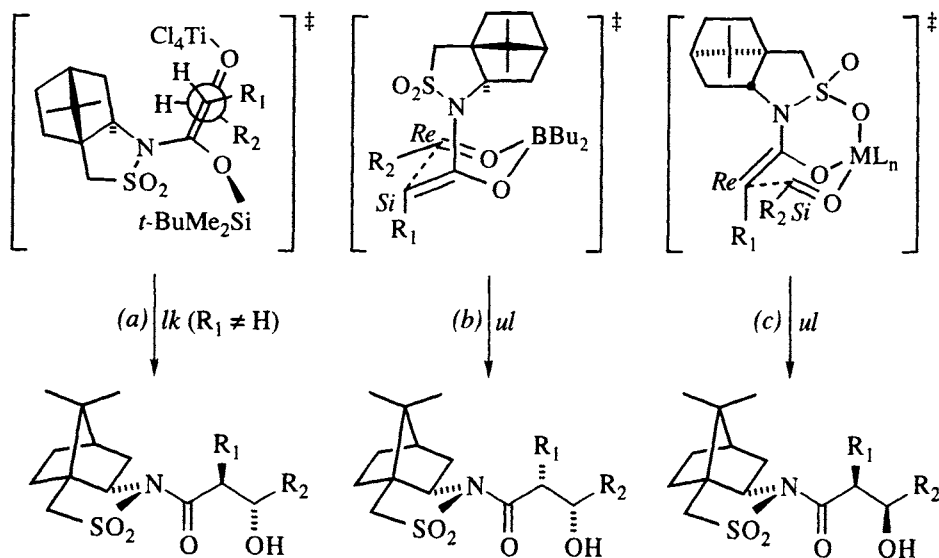
Scheme 5.13. Asymmetric addition of acetate enol silyl ethers to aldehydes [79].

Another excellent auxiliary for the asymmetric aldol addition is the camphor sultam developed in the Oppolzer laboratories (Figure 5.4e and Table 5.5). A significant feature of this auxiliary is the crystallinity of the aldol adducts, which often simplifies purification (and diastereomer enrichment). As the trimethylsilyl enol ethers (ketene acetals), acetate aldol additions afford good selectivities at -78° (Table 5.5, entry 1), and purification by recrystallization affords adducts that are >99% pure in most cases [83]. The transition structure proposed to account for the absolute configuration [83], based on an X-ray crystal structure [81], is shown in Scheme 5.14a ($R_1 = H$), and has the *tert*-butyldimethylsilyl group oriented toward the viewer (away from the camphor). Note also that the nitrogen is pyramidal and that there is little interaction between the nitrogen lone pair and the enolate double bond. With the silyl group occupying the front face, the *Re* face of the titanium-coordinated aldehyde (with the R_2 group oriented away from the camphor) approaches from the back. Approach of the aldehyde from the back is facilitated by the silyl group, which is antiperiplanar to the forming bond. A similar protocol affords anti aldolates from propionate-derived *tert*-butyldimethylsilyl enol ethers, as shown in Scheme 5.14a and entry 2 of Table 5.5 [81].

Table 5.5. Asymmetric additions of the Oppolzer sultam enolates. The "Path" column indicates the product configuration and the proposed transition structure from Scheme 5.14.

Entry	Enolate	Path	R ₂ CHO	% Yield	% ds	Ref
1		a (R ₁ =H)	Et, <i>n</i> -Bu, <i>i</i> -Pr, <i>i</i> -Bu, <i>c</i> -C ₆ H ₁₁ , Ph (& TiCl ₄)	54-75	79-96	[83]
2		a (R ₁ =Me)	Me, Et, <i>i</i> -Pr, <i>i</i> -Bu, Ph (& TiCl ₄ or ZnCl ₂)	>95	≥98	[81]
3		b (R ₁ =Me, Et, Bu)	Me, Et, <i>i</i> -Pr, <i>E</i> -crotyl, Ph	59-80	94- >99	[80]
4		c (R ₁ =Me, Et)	<i>n</i> -Pr, <i>i</i> -Pr, <i>E</i> -crotyl, Ph	31-67	65-85	[80]

ML_n=SnBu₃ or Li

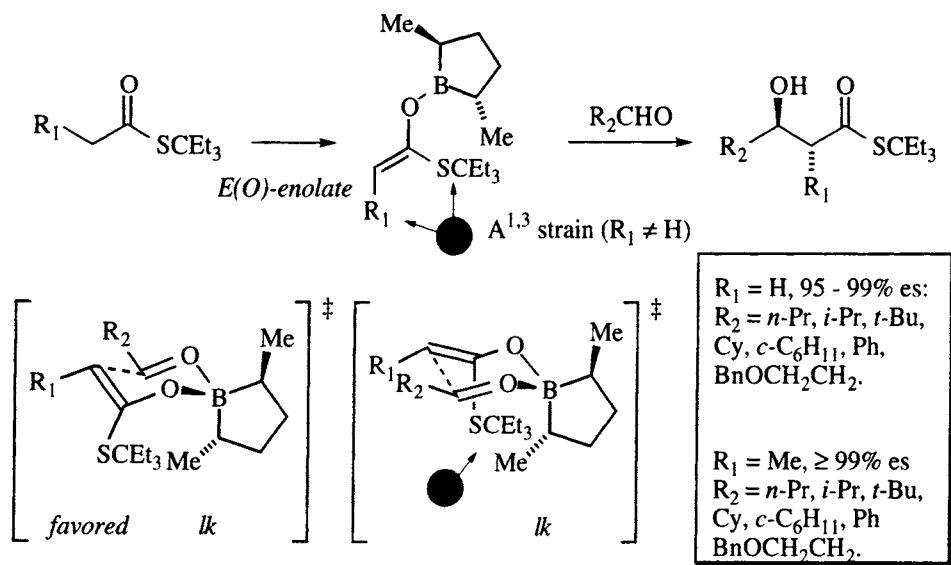
**Scheme 5.14.** Open and closed transition structures for the aldol addition of Oppolzer's sultams.

For syn aldolates, the boron enolate affords excellent selectivities and high yields [80], as shown in Table 5.5, entry 3. The rationale for the product configuration is shown in Scheme 5.14b, and is similar to the rationales presented above for other auxiliaries. Specifically, dipolar alignment of the C–O and S–O₂ bonds, coordination of the aldehyde to the boron, and approach of the aldehyde from the less hindered *Si* face in a Zimmerman-Traxler transition structure affords the absolute configuration shown. The lithium and tin enolates afford chelation-controlled syn adducts (Table 5.5, entry 4), as illustrated for the tin enolate in Scheme 5.14c. Both the lithium and the tin chelate the sultam oxygens while simultaneously coordinating the aldehyde oxygen. Addition again is thought to occur via a 6-membered chair Zimmerman-Traxler transition structure [80]. As with the Evans auxiliary, using the other enantiomer of the auxiliary is a more practical solution to changing the metal, if the syn isomer is desired.

Interligand asymmetric induction. Asymmetric induction by chiral ligands on the enolate metal has the advantage that the chiral moiety does not have to first be attached to one of the reactants and later removed (or destroyed). It is present only after enolate formation, and can be recovered for reuse. The introduction of chirality in the enolate metal (or metalloid) and its ligands is the intellectual stepping stone toward developing asymmetric catalysis for the aldol addition reaction, in that the stereogenic unit responsible for the asymmetric induction is not covalently bonded to either reactant. Additionally, chiral ligands on the metal allow double asymmetric induction when one of reactants is chiral, and triple asymmetric induction when both are. Most of the work that has been done in this area uses the same metals discussed in the previous section: boron, lithium, titanium, and tin.

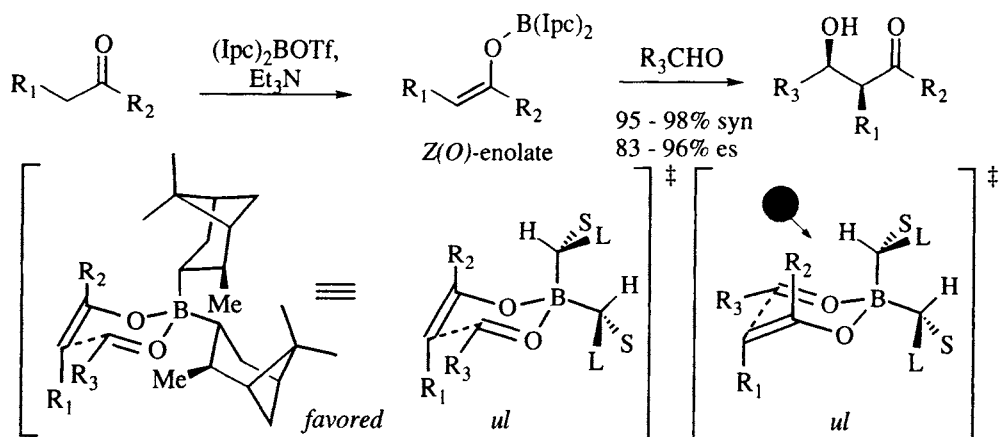
In 1986, the groups of Masamune [92] and Paterson [93] reported (virtually simultaneously) that boron enolates containing C₂-symmetric “BR₂” moieties are effective mediators in asymmetric aldol additions. The Masamune group [92] studied the aldol addition of boron esters of *tert*-heptyl thiol acetate and propionate *E*(*O*)-enolates. As shown in Scheme 5.15, both types of reagents were highly selective. When R₁ is hydrogen, the selectivities are somewhat lower, because the *tert*-heptyl group can rotate away from the C₂-symmetric boracycle. When R₁ is an alkyl group, A^{1,3} strain forces the *tert*-heptyl group toward the boracycle, crowding the transition structure and increasing the free energy difference ($\Delta\Delta G^\ddagger$) between the two illustrated transition structures. The product esters could be reduced to the corresponding primary alcohols. In spite of the high selectivities, the method has the disadvantage that the chiral boron compound is difficult to make.

Following an early lead from the Meyers group [94,95], Paterson used the readily available diisopinocampheyl (Ipc) boron triflate to make *Z*(*O*)-boron enolates of 3-pentanone [93] and other ketones [96], which add to aldehydes to produce syn adducts in 83 - 96% es (Scheme 5.16 and Table 5.6). Based on molecular mechanics calculations [55,56], the transition structure analysis shown in Scheme 5.16 was suggested to rationalize the enantioselectivity. The axial boron ligand rotates so that the C–H bond is over the top of the Zimmerman-Traxler six-membered ring, and the equatorial ligand orients with its C–H bond toward the



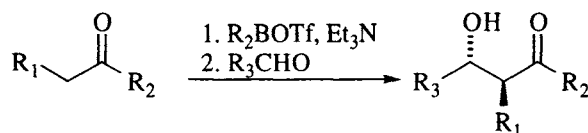
Scheme 5.15. Masamune's chiral boron enolate aldol additions [92].

axial ligand. It is interesting to note that, because of severe van der Waals interactions, the two boron-carbon bonds are conformationally locked. Note that the two methyls of the isopinocampheyl moieties are both oriented similarly, with the equatorial Ipc-methyls pointed toward the viewer. A simpler representation is to depict the carbon attached to boron as shown in the middle, with 'L' and 'S' representing the CHMe and CH₂ ligands respectively. The favored transition structure has the enolate oriented away from the 'L' ligand to avoid van der Waals repulsion between 'L' and the pseudoaxial R₂ moiety [55,56,96].



Scheme 5.16. Paterson's diisopinocampheylboron $Z(O)$ -enolate aldol addition [93,96].

Use of diisopinocampheyl boron chloride in place of the triflate affords $E(O)$ -enolates, but the isopinocampheyl ligands were ineffective for anti aldol reactions [48]. Encouraged by the molecular mechanics analysis of the $Z(O)$ -enolate additions, Gennari and Paterson used computational methods to design a new boron ligand for use with $E(O)$ -enolates [97]. The design was cued by Still's comment [98] that *cis*-2-

Table 5.6. Asymmetric aldol additions of ketone enolates using chiral ligands on boron (Ipc = isopinocampheyl; MeMn = methylmenthyl). See Schemes 5.16 and 5.17.

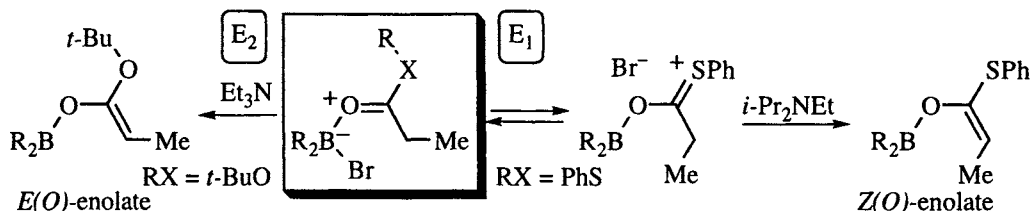
Entry	BR ₂	R ₁	R ₂	R ₃	syn:anti	% yield	% es	Ref.
1	Ipc	Me	Et	Me	97:3	91	91	[96]
2	Ipc	Me	Et	2-propenyl	98:2	78	95	[96]
3	Ipc	Me	Et	<i>n</i> -Pr	97:3	92	90	[96]
4	Ipc	Me	Et	<i>E</i> -C ₃ H ₅	98:2	75	93	[96]
5	Ipc	Me	Et	<i>i</i> -Pr	96:4	45	83	[96]
6	Ipc	Me	Et	2-furyl	96:4	84	90	[96]
7	Ipc	Me	Ph	2-propenyl	98:2	97	95	[96]
8	Ipc	Me	<i>i</i> -Pr	2-propenyl	95:5	99	94	[96]
9	Ipc	Me	<i>i</i> -Bu	2-propenyl	97:3	79	93	[96]
10	MeMn	Me	Et	2-propenyl	3:97	62	88	[97]
11	MeMn	Me	<i>i</i> -Pr	2-propenyl	0:100	51	94	[97]
12	MeMn	Me	Et	Et	8:92	50	90	[97]
13	MeMn	Me	<i>i</i> -Pr	Et	3:97	50	92	[97]
14	MeMn	Me	<i>i</i> -Pr	<i>c</i> -C ₆ H ₁₁	0:100	54	87	[97]
15	MeMn	-(CH ₂) ₃ -		2-propenyl	0:100	60	87	[97]
16	MeMn	-(CH ₂) ₄ -		2-propenyl	0:100	59	78	[97]
17	MeMn	Me	Ph	2-propenyl	14:86	60	93	[97]
18	MeMn	H	<i>i</i> -Pr	2-propenyl	—	66	88	[97]
19	MeMn	H	<i>i</i> -Bu	2-propenyl	—	80	77	[97]
20	MeMn	H	<i>t</i> -Bu	2-propenyl	—	62	88	[97]
21	MeMn	H	Me	2-propenyl	—	65	80	[97]
22	MeMn	H	Ph	2-propenyl	—	81	85	[97]
23	MeMn	H	Me	<i>n</i> -Pr	—	65	87	[97]
24	MeMn	H	Et	2-propenyl	—	51	81	[97]

In addition to their usefulness for the asymmetric addition of achiral aldehydes, it will be seen in the section 5.2.3 that the Paterson strategy is particularly useful for the aldol addition of chiral fragments such as the large, polyfunctional ketone and aldehyde fragments needed for convergent macrolide synthesis.

In 1989, Corey reported that diazaborolidines are efficient reagents for asymmetric aldol additions of acetate and propionate thioesters [99]. Thioesters add to aldehydes giving syn adducts, whereas *tert*-butyl esters give anti adducts [100]. Both react via closed, Zimmerman-Traxler transition states; the difference in the topicity is due to different enolate geometries for the two ester types. Corey's rationale for the divergent enolate geometries involves competing mechanisms for deprotonation of the zwitterion shown in Scheme 5.18. Complexation of the boron reagent with the ester produces the zwitterionic complex (boxed), which may undergo either E₁ or E₂ elimination of HBr. Ionization (E₁) is favored when RX is

thiophenyl and disfavored when RX is *tert*-butoxy; E₁ is also favored when the base is bulky, while smaller bases facilitate E₂ reaction. Note that E₁ ionization can only occur when X can easily stabilize the positive charge by resonance, which is only possible when the substituent on X (R) becomes coplanar with the rest of the molecule. Deprotonation by an E₂ mechanism is faster with the less bulky triethyl amine than with diisopropylethyl amine. Corey suggests that both E₁ and E₂ reactions occur from the illustrated conformation of the zwitterion [100].

For esters, deprotonation is effected with triethyl amine (which favors E₂), while E₁ ionization is disfavored because it requires moving the bulky *tert*-butyl group into planarity. For thioesters, E₁ reaction is facilitated by the thiophenyl group, while E₂ reaction is slowed by use of the bulky diisopropyl ethyl amine.¹¹

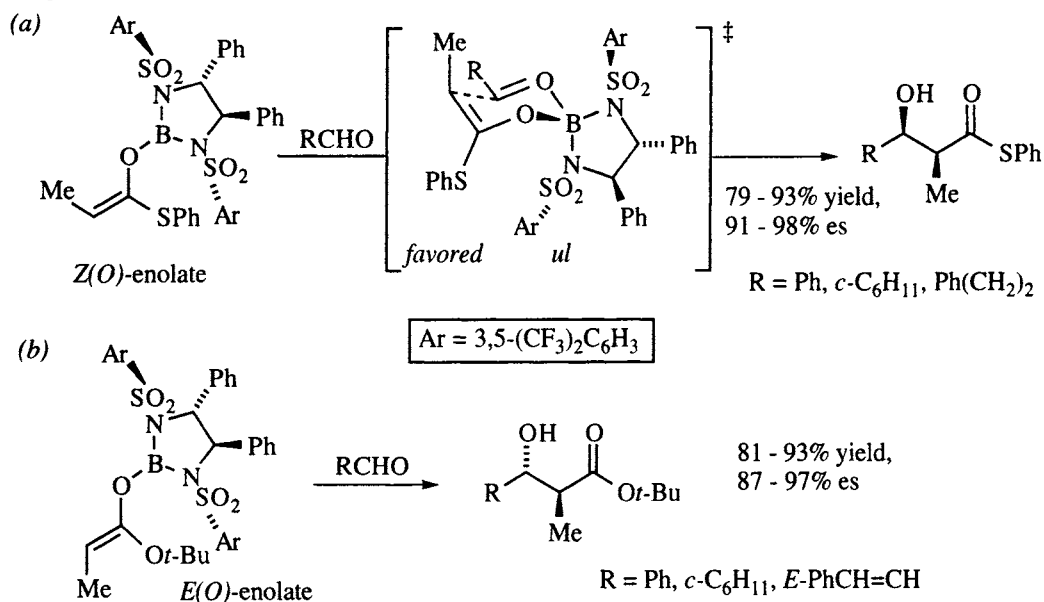


Scheme 5.18. Rationale for boron enolate stereochemistry [100].

The diazaborolidines mediate the diastereoselective and enantioselective formation of *syn* [99,100] *anti* aldols [100], as summarized in Scheme 5.19. The aryl group of the sulfonamide must be electron withdrawing, or else the boron is not a strong enough Lewis acid to mediate the process. The process has also been used for the formation of *anti* halohydrins [102,103], and in aldol additions to azomethines [101]. The illustrated transition structure (Scheme 5.19a) has been postulated to account for the observed enantioselectivity in the *Z(O)*-enolate addition [99]. Corey suggests that the *trans* phenyl substituents force the sulfonamide aryl groups into a conformation that places each aryl ring in a *trans* orientation to its neighbor. This *conformation* is reminiscent of the *configuration* engineered by Masamune earlier (Scheme 5.15), and may have similar control features. It is interesting to note, however, that a similar chair transition structure employing the *E(O)*-enolate predicts the wrong enantiomer (Scheme 5.19b) of the *anti* addition product [104]!

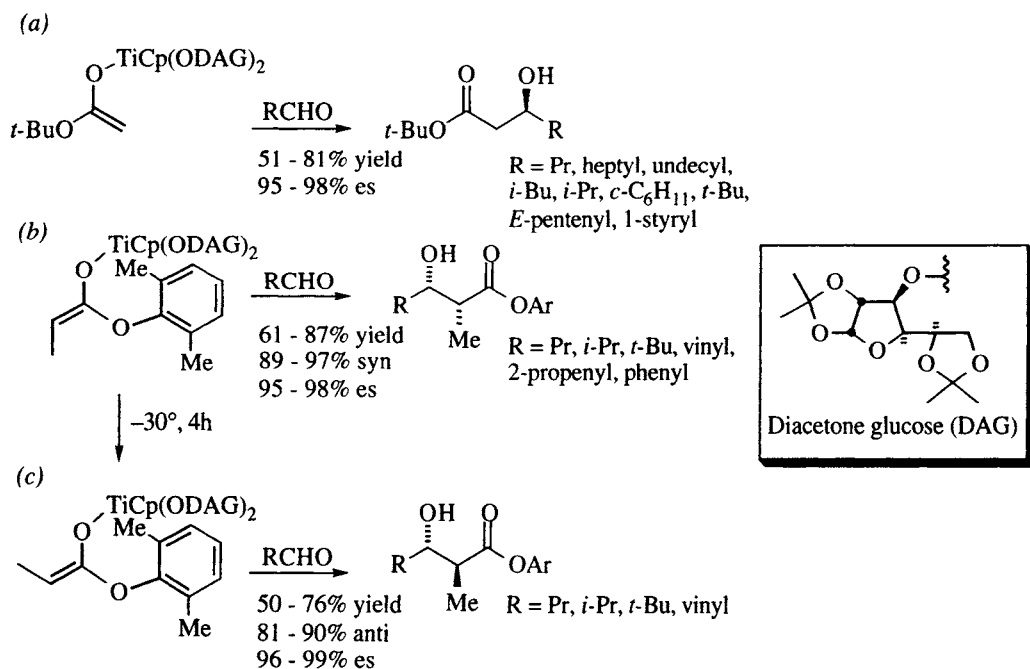
Duthaler and colleagues have used diacetone glucose as a ligand on titanium to induce enantioselectivity in the addition of acetate and propionate enolates (Scheme 5.20 [105,106]. The most interesting feature of the addition of the titanium enolate of *tert*-butyl acetate (Scheme 5.20a) is that the best selectivities were achieved at room temperature, making this procedure one of the most promising for scaleup [105]. Deprotonation of 2,6-dimethylphenyl propionate gives the *E(O)*-enolate, which is transmetalated slowly to the titanium enolate at -78° [106]. Addition to a

¹¹ A rationale similar to this may be used to explain the selective formation of *E(O)*-enolates of *tert*-heptylthio- and *tert*-butylthiopropionates (Scheme 5.15 and ref. [101]): the Et₃CS[−] replaces the Me₃CO[−] in the Scheme 5.18 rationale) and the selective formation of ketone *Z(O)*-enolates with dialkyl boron triflates and *E(O)*-enolates with dialkylboron halides (Scheme 5.16 and 5.17: the triflates are more likely to ionize than the halides, thus favoring ionization over direct deprotonation of the zwitterion).



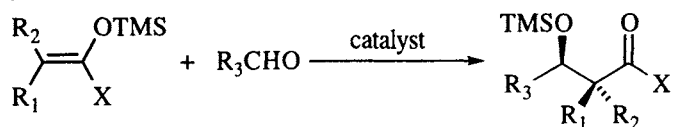
Scheme 5.19. Corey's diazaborolidine-mediated aldol additions [99,100].

number of aldehydes affords predominantly syn adducts in excellent diastereo- and enantioselectivities. Warming the titanium enolate to -30° results in isomerization to the *Z(O)*-enolate, which adds to aldehydes with varying degrees of diastereo-selectivity. Some of the more selective examples are shown in Scheme 5.20b. Note that these examples are an exception to the generalization that *Z(O)*-enolates afford syn



Scheme 5.20. Duthaler's diacetone glucose titanium enolate aldol additions [105,106].

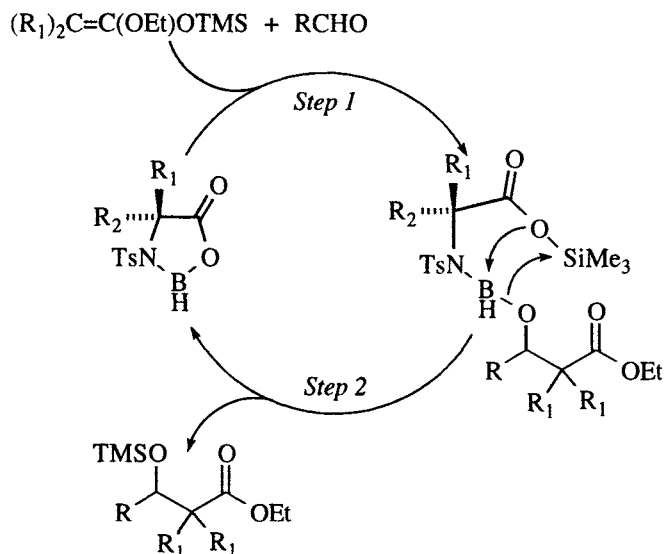
adducts and *E(O)*-enolates afford anti adducts. The authors suggest a boat transition structure to account for the fact (*cf.* Figure 5.3b), but do not speculate on the conformation of the diacetone glucose ligands and do not suggest a model to account for the chirality sense of the product. Finally, a single example (not illustrated here) of a *Z(O)*-enolate of an (achiral) oxazolidinone propionimide was reported to add to isobutyraldehyde in 50% yield, 88% diastereoselectivity (anti), and 97% enantioselectivity [106]. Other groups have examined chiral diamine ligands on achiral tin [107] and lithium enolates [108, 109], but the selectivities are not as high as reported

Table 5.7. Catalytic Mukaiyama aldol additions. The catalyst column refers to the structures in Figure 5.6

Entry	Catalyst (mole %)	R ₁ , R ₂	X	R ₃	% Yield	% es	Ref.
1	a (100)	Me, Me	OEt	Ph, <i>E</i> - PhCH=CH-, Ph(CH ₂) ₂ -	80-87	91-96	[112]
2	a (20)	Me, Me	OEt	<i>i</i> -Pr, Ph, <i>E</i> - PhCH=CH-, Ph(CH ₂) ₂ -	60-97	91-98	[113]
3	a (20)	H, H	OPh	Ph	66	90	[113]
4	b (17)	Me, Me	OEt	<i>n</i> -Pr, <i>i</i> -Bu, Ph, <i>c</i> -C ₆ H ₁₁ , Ph(CH ₂) ₂ -, BnO(CH ₂) ₂ -	68-86	92-99	[114]
5	c (20)	H, H	<i>n</i> -Bu, Ph	<i>n</i> -Pr, <i>c</i> -C ₆ H ₁₁ , 2-furyl, Ph	56-100	93-96	[115]
6	d (20)	H, Me (<i>E</i> , <i>Z</i> mix)	Et, <i>n</i> -Bu, Ph	<i>n</i> -Pr, <i>n</i> -Bu, <i>E</i> -CH ₃ CH=CH-, <i>E</i> -PhCH=CH-, Ph	55-99 (80 - >95% syn)	77-96	[116]
7	e (100)	H, H	SEt	<i>i</i> -Pr, <i>t</i> -Bu, Ph, Ph(CH ₂) ₂	77-90	91-99	[118]
8	f (100)	H, H	SEt	<i>i</i> -Pr, <i>i</i> -Bu, Ph, <i>c</i> -C ₆ H ₁₁ , <i>n</i> -C ₇ H ₁₅ , <i>E</i> -PhCH=CH-, <i>E</i> -MeCH=CH-, Ph(CH ₂) ₂ -	70-96 (100% syn)	>99	[118]
9	f (20)	Me, H	SEt	<i>n</i> -C ₅ H ₁₁ , Ph, <i>c</i> -C ₆ H ₁₁ , <i>E</i> -PhCH=CH-, <i>E</i> -MeCH=CH-	67-80 (80-100% syn)	94-99	[121]

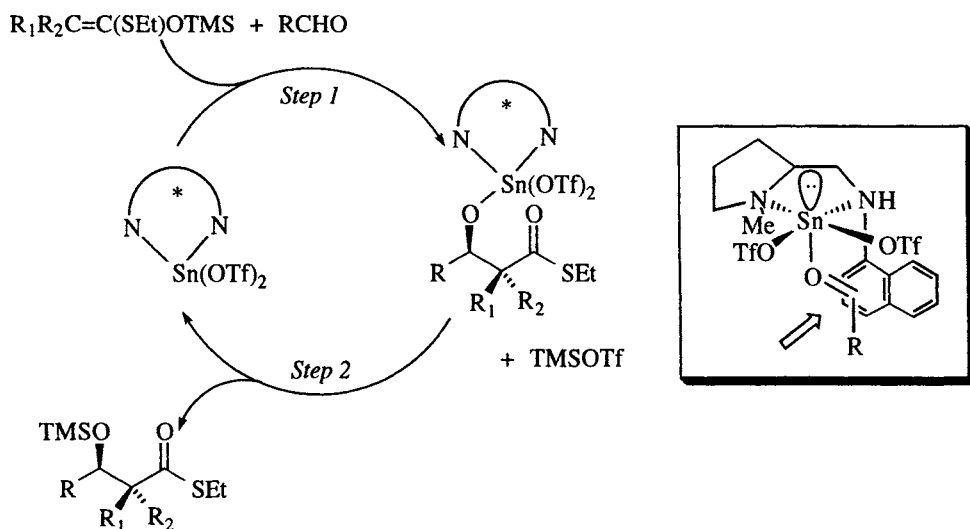
An interesting point is the difference between the Masamune (Figure 5.6b) and Kiyooka (Figure 5.6a) catalysts. One is catalytic and the other is not (Table 5.7, entries 1 and 4). Masamune screened a number of catalysts, including ones similar to Kiyooka's (Figure 5.6a), and suggested the catalytic cycle illustrated in Scheme

5.21, in which step two is thought to be the slow step. The critical difference is the quaternary stereocenter in the Masamune catalyst ($R_2 \neq H$). When the stereocenter in the catalyst is quaternary, the N–C–CO bond angle is compressed (Thorpe–Ingold effect – see glossary, section 1.6), thereby accelerating the silicon transfer (note the cyclic transition state) so that the catalyst can turn over more efficiently.



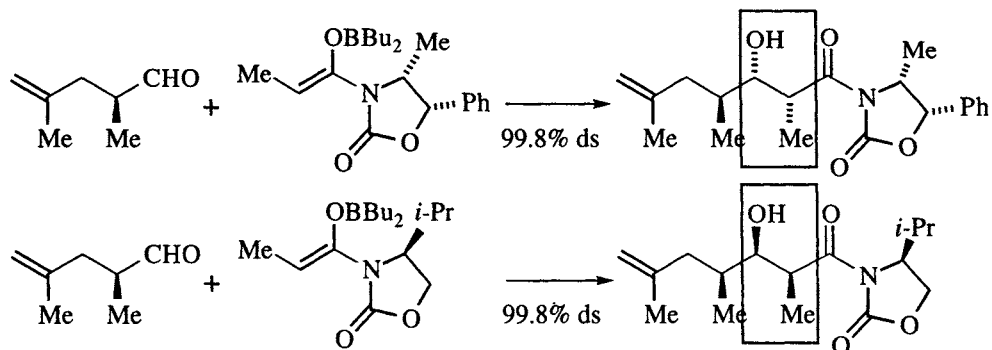
Scheme 5.21. Catalytic cycle for oxazaborolidine catalyzed Mukaiyama aldol addition (after ref. [115]).

Another catalytic system has been developed by Kobayashi and Mukaiyama. Specifically, tin triflates ligated by chiral diamines (Figure 5.6e,f) activate aldehydes toward addition by silyl enol ethers of acetate and *E(O)*-propionate thioesters (Table 5.7, entries 7–9). The catalytic version is thought to go by the two-step process shown in Scheme 5.22, with the slow step again being release of the alk-



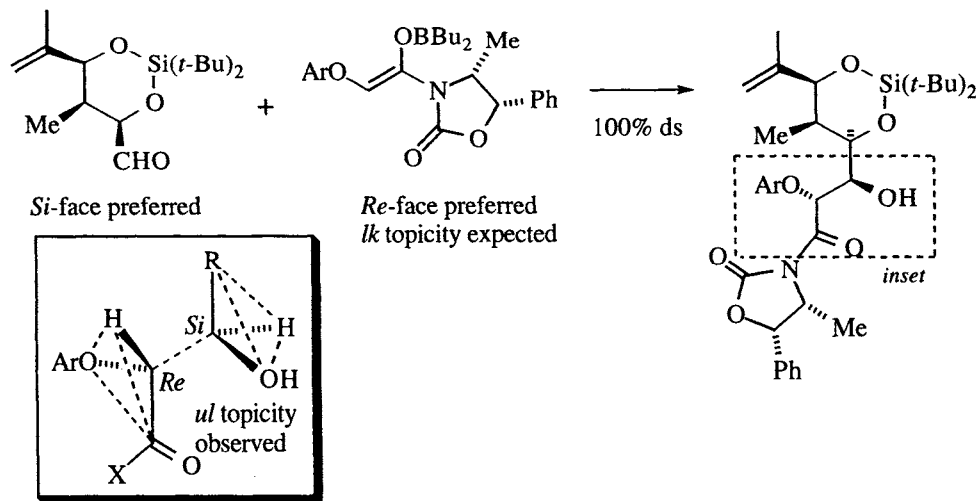
Scheme 5.22. Proposed catalytic cycle for the Kobayashi-Mukaiyama aldol addition. Inset: proposed model for the aldehyde *Si*-face selectivity due to the catalyst [121,122].

oxide adduct by silylation [121,122]. Polar solvents such as propionitrile improve the catalytic process, presumably by increasing the rate of step two [121]. The rationale for the *Si*-face selectivity for the aldehyde is shown in the inset [122], however the authors did not postulate a transition structure to rationalize the topicity. It is clear that the mechanism does not involve silicon-tin enolate exchange [118], however unlike many acid catalyzed aldol additions, both the rate and the selectivity of the addition are dependent on enolate geometry. For the examples in



Scheme 5.24. Reagent-based stereocontrol in aldol additions using Evans imide enolates [125].

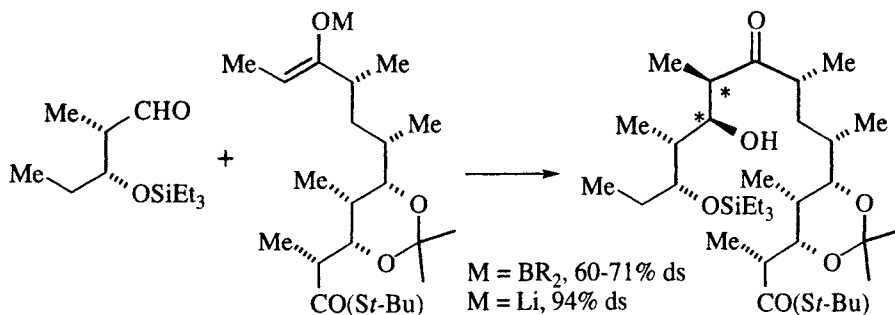
One cannot always bank on reagent-based stereocontrol, even with reagents as selective as the Evans imide enolates. For example, during the course of a synthesis of cytovaricin [126], the enolate shown in Scheme 5.25 was expected to afford the syn adduct when added to the aldehyde illustrated. Instead, an anti aldol adduct was formed as a single diastereomer. Note that the *Re* face of the enolate is preferred according to the transition state analysis presented in Scheme 5.12a, and the *Si* face of the aldehyde is preferred according to the Felkin-Anh theory (section 4.1 and Figure 4.8 or see glossary, section 1.6). Analysis of the product configuration, as shown in the inset, indicates that the preferred faces of both the enolate and aldehyde were coupled. Apparently, the *Si* facial preference of the aldehyde was sufficiently strong to disrupt the *lk* topicity preferred by the enolate.



Scheme 5.25. A rare case of mismatched double asymmetric induction that is 100% diastereoselective [126].

Although the asymmetric addition of propionate enolates (outlined above) is a valuable synthetic tool, its use is restricted to targets that are amenable to a linear synthetic plan. Aldol additions may also be used to couple two large fragments in a convergent synthesis, but such reactions are not amenable to auxiliary based

approaches. This weakness was recognized early in the development of the asymmetric aldol methodologies. For example, in the synthesis of 6-deoxyerythronolide B, the Masamune group assembled two fragments that were coupled with a poor selectivity (60-71% ds) using boron enolates (Scheme 5.26). Switching to a lithium enolate increased the selectivity to 94%, but considerable background work had to be undertaken to insure success [127,128]. This result is somewhat surprising since boron enolates are typically more selective than lithium enolates.



Scheme 5.26. Selective coupling of two chiral fragments (double asymmetric induction) in the asymmetric synthesis of 6-deoxyerythronolide B [124,127]. For a similar reaction in the synthesis of erythronolide B, see ref. [129].

Analysis of the major addition product of Scheme 5.26 (Figure 5.7a) indicates that the *Si* face of the enolate adds to the *Re* face of the aldehyde; the latter corresponds to anti-Cram selectivity (section 4.1). Two explanations have been offered to explain the selectivity of this aldehyde. Masamune originally suggested that the enolate adds to the aldehyde through a boat transition state that is also chelated by the silyloxy group (Cram cyclic model, section 4.2), as illustrated in Figure 5.7b. Weaknesses of this postulate are that Cram's cyclic model is more often effective when the chelate is a five-membered ring, and that the triethylsilyloxy group probably is not a good chelator [130]. Ten years after Masamune's original hypothesis was offered, Roush analyzed a considerable amount of data accumulated in the interim, and pointed out that a Zimmerman-Traxler chair, adding to the *Si* face of the aldehyde (as expected by the Felkin-Anh model), is de-

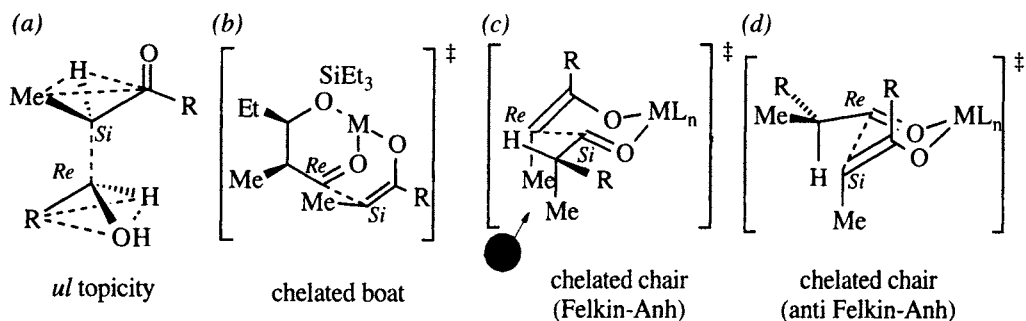


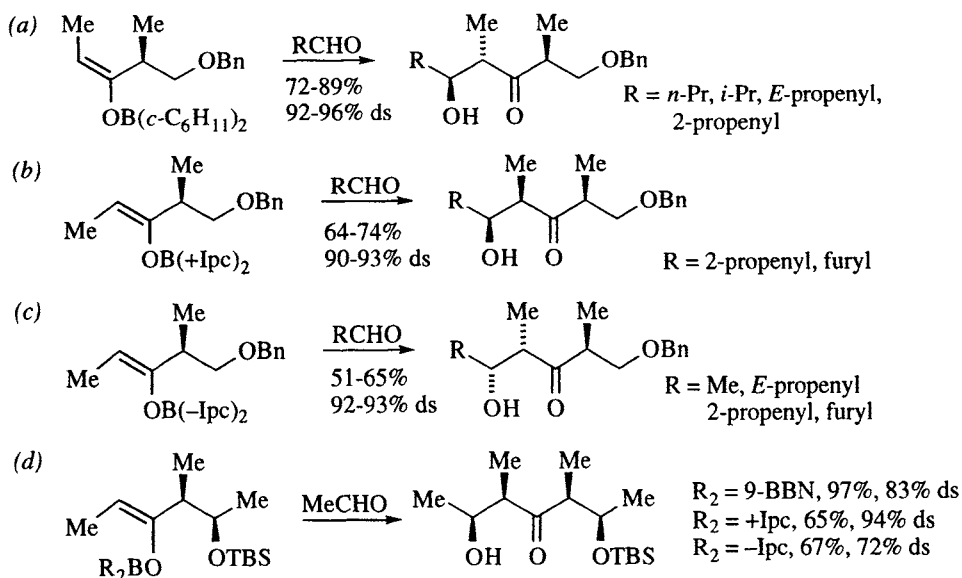
Figure 5.7. Analysis of possible transition structures for the aldol addition in Scheme 5.26: (a) The observed topicity; (b) boat transition structure postulated by Masamune [127]; (c) gauche pentane interaction that destabilizes the Cram (or Felkin-Anh) selectivity of the aldehyde; (d) anti-Cram (anti Felkin-Anh) addition via a chelated chair [123].

stabilized by a 2,3-*P*,3,4-*M* gauche pentane interaction (*cf.* Figure 5.5), as indicated in Figure 5.7c. Roush suggests that an anti Felkin-Anh (anti-Cram) chair transition structure more adequately explains the facts, as shown in Figure 5.7d [123].

Whatever the mechanism, achiral lithium enolates add to the aldehyde of Scheme 5.26 with selectivities in the 80-90% *ds* range; the higher selectivity observed with the chiral enolate may therefore be attributed to matched pair double asymmetric induction [127]. However, note that if the target had had the opposite absolute configuration at the indicated stereocenters, it would have been the minor isomer under any of the conditions examined.

The stereoselectivity of the aldol additions shown in Schemes 5.25 and 5.26 are obviously the result of a complex series of factors, among which are the Felkin-Anh preference dictated by the α -substituent on the aldehyde, the proximal stereocenters on the enolate, etc. Additionally, the more remote stereocenters, such as at the β -position of the aldehyde, may influence the selectivity of these types of reactions. Evans has begun an investigation into some of the more subtle effects on crossed aldol selectivity, such as protecting groups at a remote site on the enolate [131], and of β -substituents on the aldehyde component [132], and also of matched and mismatched stereocenters at the α and β positions of an aldehyde (double asymmetric induction) [133]. Further, the effect of chiral enolates adding to α,β -disubstituted aldehydes has been evaluated [134]. The latter turns out to be a case of triple asymmetric induction, with three possible outcomes: fully matched, partially matched, and one fully mismatched trio.

Another approach to the aldol problem has been investigated in the Paterson laboratory, in the hopes of using interligand asymmetric induction to control absolute configuration of the new stereocenters in the products [48,135,136]. Some examples are shown in Scheme 5.27. The chiral *E*(*O*)-enolate shown in Scheme



Scheme 5.27. (a) Anti-selective addition of ketone *E*(*O*)-enolate to aldehydes [137,138]; (b, c) Reagent controlled addition of *Z*(*O*)-enolate to aldehydes [126]; (d) Double asymmetric induction where the mismatched diastereoselectivity is decreased, not reversed [139].

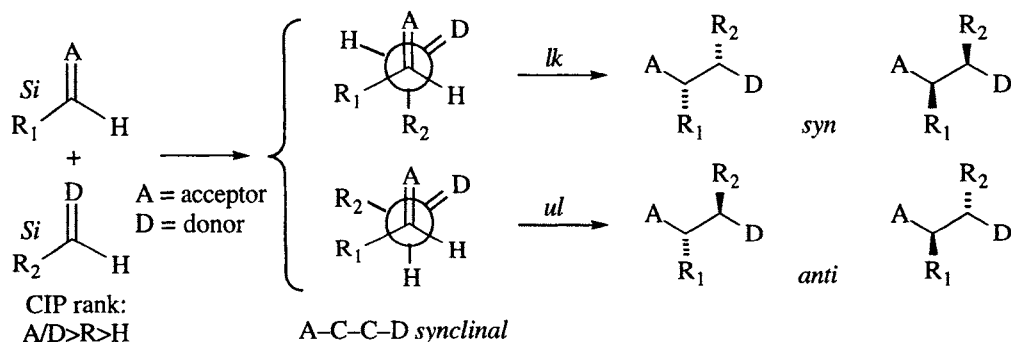
5.26a adds to simple achiral aldehydes in high yield and with 95-96% diastereoselectivity [137]. In contrast, the *Z(O)*-enolate having achiral boron ligands, of this and similar chiral ketones, affords poor selectivity in aldol additions [126,137,138], probably because of gauche pentane interactions similar to those illustrated in Figure 5.7c. Double asymmetric induction via chiral ligands on boron can sometimes be used to control the configuration of the aldol adducts. As shown in Scheme 5.27b and c, either (+) or (-) isopinocampheyl (Ipc) ligands on boron (*cf.* Scheme 5.16) control the absolute configuration of the addition products for the enolate shown [126]. The Ipc ligands cannot always be relied upon to control

5.3 Michael additions¹⁴

The term “Michael addition” has been used to describe 1,4- (conjugate) additions of a variety of nucleophiles including organometallics, heteroatom nucleophiles such as sulfides and amines, enolates, and allylic organometals to so-called “Michael acceptors” such as α,β -unsaturated aldehydes, ketones, esters, nitriles, sulfoxides, and nitro compounds. Here, the term is restricted to the classical Michael reaction, which employs resonance-stabilized anions such as enolates and azaenolates, but a few examples of enamines are also included because of the close mechanistic similarities.

5.3.1 Simple diastereoselectivity

When a prochiral acceptor ($R_1CH=A$) and a prochiral donor ($R_2CH=D$) react, the stereoisomers are labeled as either *syn* or *anti* based on the relative configurations of R_1 and R_2 when the Michael adduct is drawn in a zig-zag projection, as shown in Scheme 5.28. Using the *Re/Si* nomenclature and assuming that the CIP rank is $A > R_1 > H$ and $D > R_2 > H$, the *syn* adducts arise from *lk* topology and *anti* adducts arise from *ul* topology.



Scheme 5.28. Topicity [6,57] and adduct [148] nomenclature for Michael additions.

Seebach suggested in 1981 [57] that the donor and acceptor are probably synclinal in the transition state. Steric repulsion between R_1 and the donor, D , is proposed to orient R_1 antiperiplanar to D ; pyramidalization (*cf.* Figure 3.4 and *ref.* [150-153]) and tilting of the donor to accommodate the Bürgi-Dunitz angle of 107°

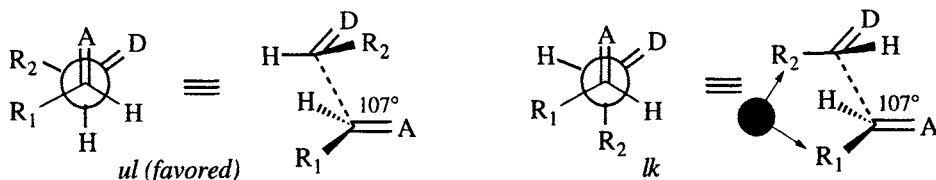
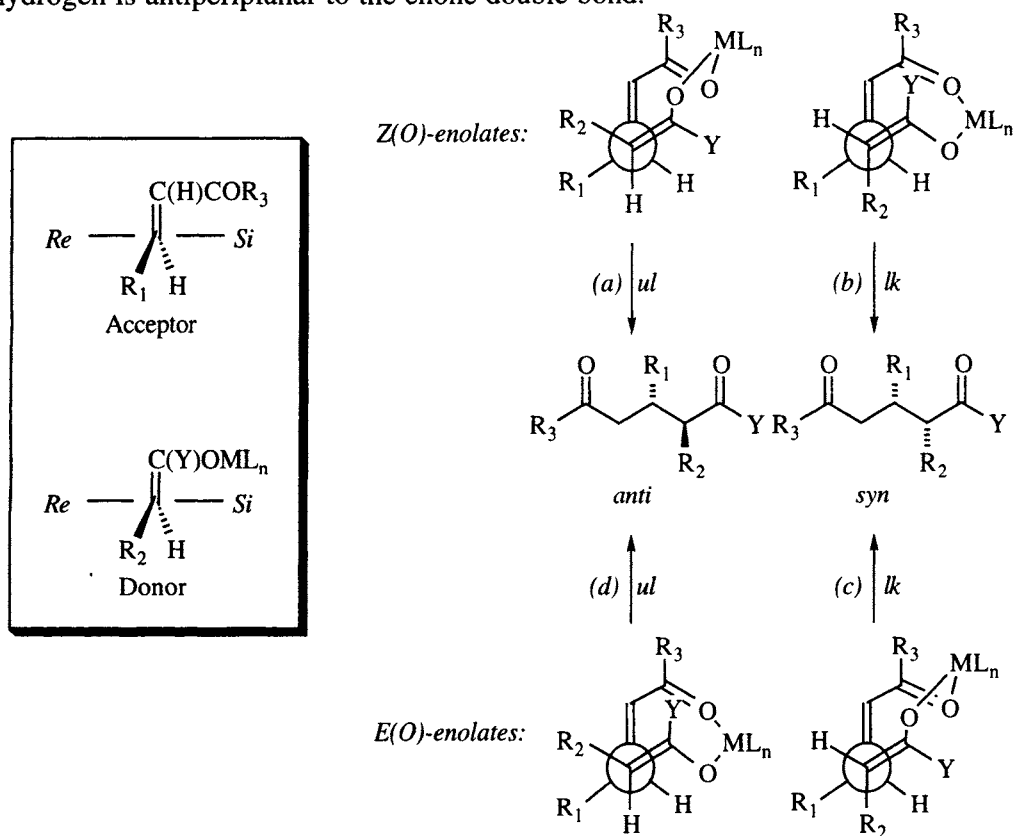


Figure 5.9. Pyramidalization of the donor and the Bürgi-Dunitz trajectory contribute to destabilization of the *lk* topology combination according to Seebach [57].

¹⁴ For a comprehensive coverage of conjugate addition reactions, see *ref.* [147]. For a comprehensive review of the stereochemical aspects of base-promoted Michael reaction, see *ref.* [148]; for a similarly comprehensive review of acid-catalyzed Michael reactions and conjugate additions of enamines, see *ref.* [149].

(cf. Figures 4.6, 4.7, and ref. [154-156]) are proposed to disfavor the *lk* topology, since R_2 is more sterically demanding than hydrogen (Figure 5.9).

Analysis of numerous examples [148,149] and mechanistic studies [157,158] led Heathcock to refine these hypotheses and, in consideration of the actual substituents (R_1 , R_2 , A, and D), place them on firmer mechanistic grounds.¹⁵ The four transition structures in Scheme 5.29 are direct extensions of those in Scheme 5.28 and Figure 5.9. For ketone and ester enolates, there is a strong correlation between the relative configuration of the product and the enolate geometry: *Z(O)*-enolates give anti products and *E(O)*-enolates give syn adducts [157]. The rationale for this is that transition structures for paths a and c (Scheme 5.29) are favored due to repulsive interactions between Y and R_3 in paths b and d. The selectivity of *Z(O)*-enolates appears to be higher than that of *E(O)*-enolates, probably due to the destabilization of path c by the pyramidalization and trajectory considerations illustrated in Figure 5.9, which intrinsically favor paths a and d, in which a hydrogen is antiperiplanar to the enone double bond.



Scheme 5.29. Proposed chelated transition structures (and topicities) for Michael additions of lithium enolates of ketones, esters, and amides to enones [157,158]. Only one enantiomeric transition structure and product is shown for each topology (*Si* face of the acceptor).

¹⁵ On the other hand, a computational study [159] of the Michael addition of propionaldehyde lithium enolate adding to *E*-crotonaldehyde indicates an anticlinal conformation around the forming bond (*i.e.* A eclipsing R_2 in the *ul* topology and A eclipsing H in the *lk* topology of Figure 5.9).

For amide enolates, the situation is similar in that, when R_3 and Y are large, the transition structures of paths a and c are favored [158]. However, recall that acyclic amides invariably form $Z(O)$ -enolates, so amide $E(O)$ -enolates are only possible when R_2 and Y are joined: *i.e.*, in a lactam. In contrast to ketone and ester enolates, however, the transition structures of paths b and d appear to be intrinsically favored when Y and R_3 are small. This latter trend is (at least partly) contrary to what would be expected based on the simple analysis of Figure 5.9, but can be rationalized as follows. For the lactams, the R_2 and Y substituents present a rather flat profile, so that interaction with R_3 in path d is minimal. Additionally, the R_2 - Y ring 'eclipses' the β -hydrogen of the enone in c, destabilizing this structure. For amide $Z(O)$ -enolates and acceptors with an R_3 substituent such as a phenyl, there may actually be an attractive interaction between Y and R_3 , favoring path b.

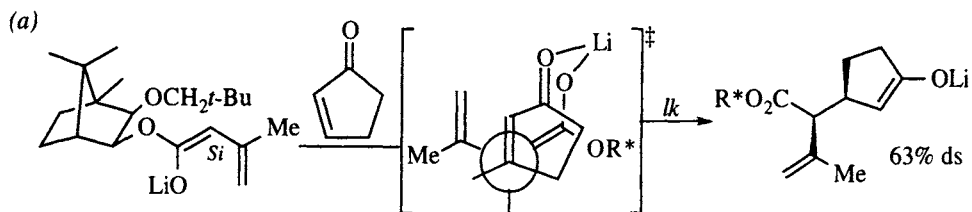
Clearly each case must be analyzed separately, but these transition structures serve as a starting point for such analyses. Note also that the structures of Scheme 5.29 all have enones in an *s-cis* conformation, which is not available to cyclic acceptors such as cyclohexenone, cyclopentenone, and unsaturated lactones.

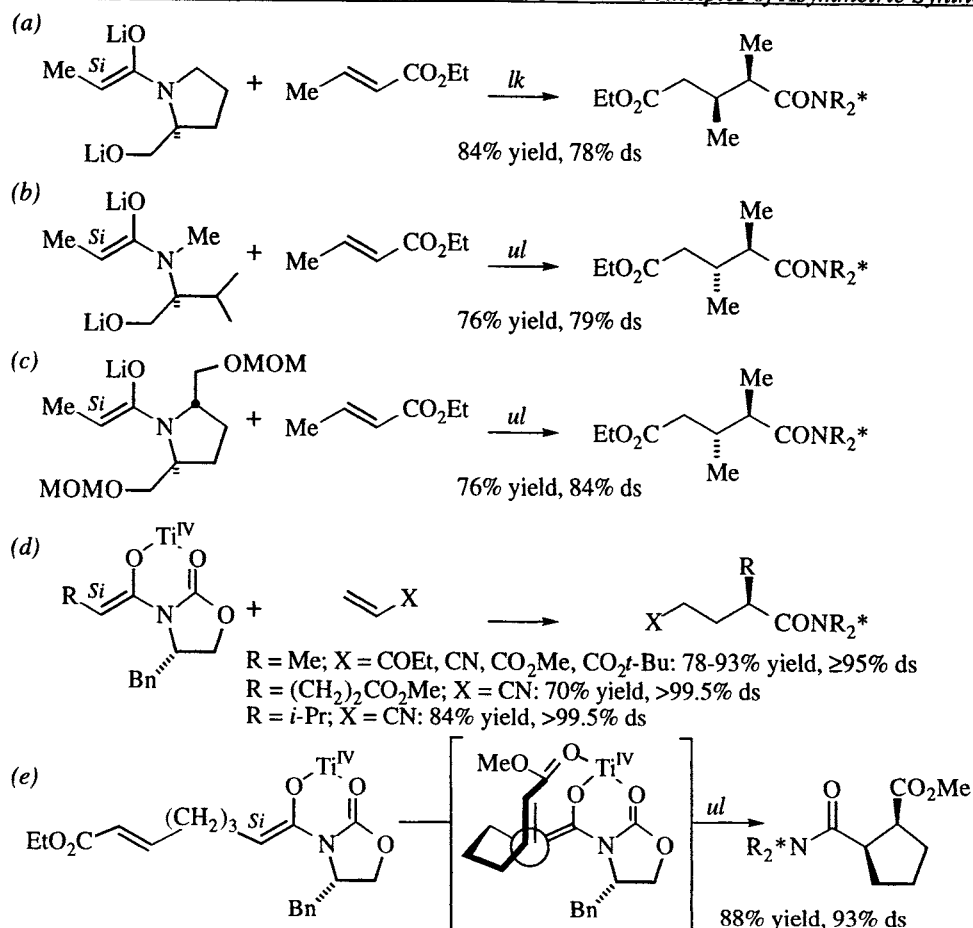
For the purpose of asymmetric synthesis, we are interested in expanding on simple diastereoselectivity and differentiating between the two *ul* transition structures (*Re-Re* and *Si-Si*) and the two *lk* transition structures (*Re-Si* and *Si-Re*) for each enolate geometry. This is done by rendering the *Re* and *Si* faces of either component diastereotopic by the introduction of a stereogenic element. For asymmetric Michael reactions, a stereocenter in a removable substituent on the acceptor or in Y or the metal (ML_n) of the donor have been used to this end. Introduction of stereogenicity in substituents on the donor or the acceptor constitute auxiliary-based approaches, while a chiral ligand on the metal is interligand asymmetric induction. The following discussion is organized by the location of the stereogenic unit. Given the number of chiral enolate reagents developed for asymmetric alkylations and aldol additions, it should come as no surprise that many of these auxiliaries have also found use in Michael additions.

5.3.2 Chiral donors

Ester enolates. Oppolzer showed in 1983 that the $Z(O)$ -dienolate shown in Scheme 5.30a adds to cyclopentenone with 63% diastereoselectivity [160]. Additionally, the enolate adduct can be allylated selectively, thereby affording (after purification) a single stereoisomer having three contiguous stereocenters in 48% yield. The transition structure illustrated is not analogous to any of those illustrated in Scheme 5.29 because cyclopentenone is an *s-trans-Z*-enone, whereas the enones in Scheme 5.29 are *s-cis-E*. In 1985, Corey reported the asymmetric Michael addition of the $E(O)$ -enolate of phenylmenthone propionate to *E*-methyl crotonate as shown in Scheme 5.30b [161]. The product mixture was 90% syn, and the syn adducts were produced in a 95:5 ratio, for an overall selectivity of 86% for the illustrated isomer. The transition structure proposed by the authors to account for the observed selectivity is similar to that shown in Scheme 5.29c, but with the enone illustrated in an *s-trans* conformation. Intramolecular variations of these reactions were reported by Stork in 1986, as illustrated in Scheme 5.30c and 5.29d [162]. Two features of

these reactions deserve comment. First, the carbonyl of the acceptor is not chelated to the enolate metal, and second, the selectivity of the camphor-derived ester is significantly higher than the similar reaction in Scheme 5.30a. The latter effect seems to be due to the position of the bridgehead methyl, which helps restrict conformational motion when it neighbors the ester enolate [162]. Note that hydrolysis of the adducts from these two reactions afford enantiomeric cyclopentanones.



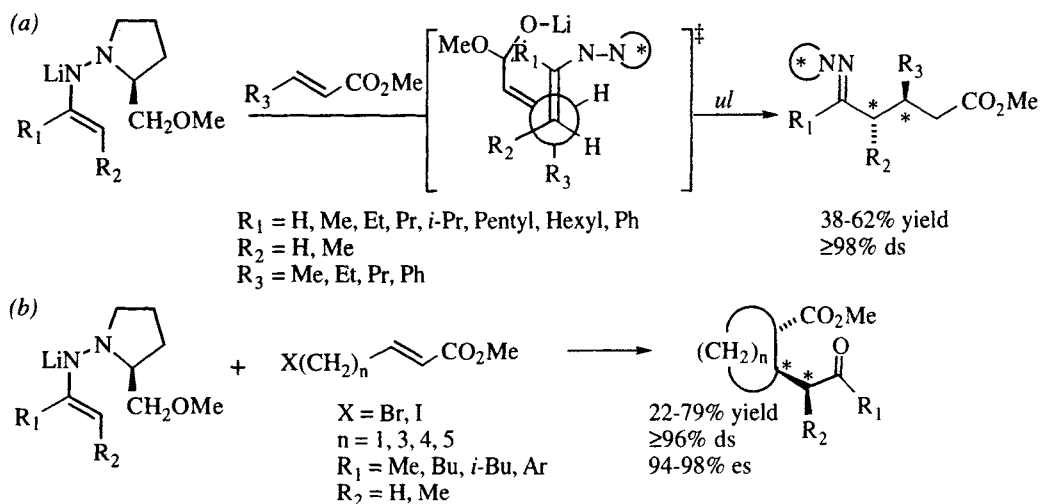


Scheme 5.31. Asymmetric Michael addition of amide and imide enolates. (a-c) [163]. (d) [164], [165]. (e) [165].

These four examples do not seem to comply with a consistent mechanistic model. The dilithioprolinol amide enolate in Scheme 5.31a is attacked on the enolate *Si* face, in accord with the sense of asymmetric induction observed in alkylations of this enolate [166,167]. On the other hand, the structurally similar dilithiovalinol amide enolate, while being attacked on the same face (as expected), reverses topicity. Furthermore, the *S,S*-pyrrolidine enolate in Scheme 5.31c is attacked from the *Si* face by Michael acceptors, but from the *Re* face by alkyl halides [168] and acid chlorides [169]. The titanium imide enolate in Scheme 5.31d adds Michael acceptors from the *Si* face, consistent with the precedent of aldol additions of titanium enolates (*cf.* Table 5.4, entry 2, [88]). An intramolecular addition (Scheme 5.31e) seems to follow a clear mechanistic path [165]: the *Si* face is attacked by the electrophile, and the *cis* geometry of the product implicates intramolecular complexation of the acceptor carbonyl. This coordination of the acceptor carbonyl is probably a function of the metal: recall the lithium ester enolates illustrated in Scheme 5.30c and d, but also metal chelation in titanium aldol additions (Table 5.4, entry 2).

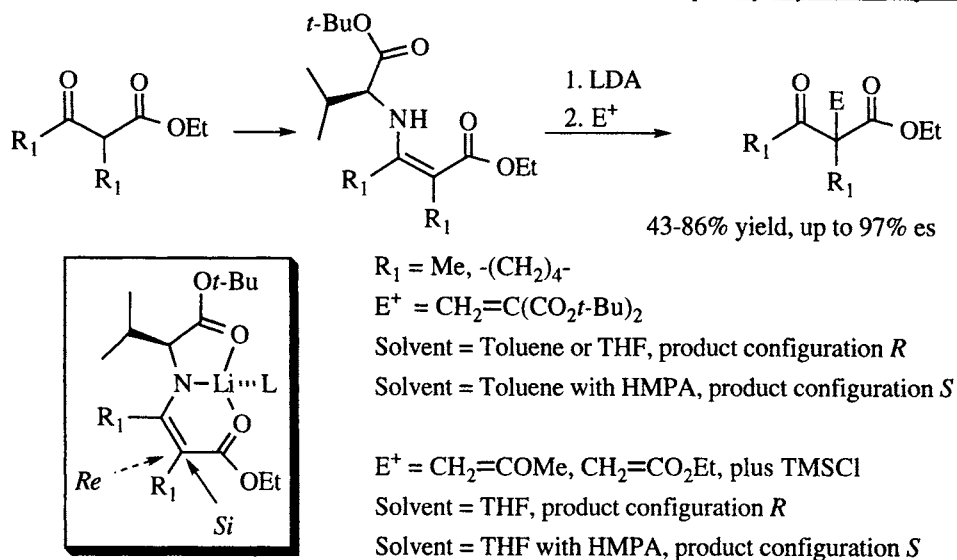
Ketone and aldehyde azaenolates. Perhaps the most versatile of the auxiliaries for the asymmetric alkylation of ketones and aldehydes are the SAMP/RAMP hydra-

zones developed by Enders (cf. Schemes 3.21, 3.22, and Table 3.9). These hydrazones, as their lithium *E(O)*-enolates, also undergo highly selective Michael additions [170-173]. Several examples are illustrated in Scheme 5.32a. The rationale for the formation of the *E(O)*-enolate and for the *Re* facial selectivity of SAMP hydrazones is illustrated in Scheme 3.22. The Michael acceptors also react on the *Re* face of SAMP hydrazones, and the *ul* topology at the new bond can be rationalized by Seebach's postulate (Figure 5.9 and Scheme 5.29d), that places the β -substituent of the Michael acceptor (R_3 in Scheme 5.32a) antiperiplanar to the double bond of the donor ($=D$ in Figure 5.9), and has the acceptor double bond ($=A$ in Figure 5.9) bisecting the angle between the donor double bond ($=D$) and the donor substituent (R_2 in Scheme 5.32a). Scheme 5.32b illustrates an extension for the synthesis of substituted cycloalkanes. The indicated (*) stereocenters are formed in the Michael addition; in Scheme 5.32b, the other is formed by internal 1,2-asymmetric induction.



Scheme 5.32. Michael additions of SAMP/RAMP hydrazones. (a) [170-172]. (b) [173]. Stereocenters formed in the Michael reaction are indicated (*).

The Koga group has investigated the asymmetric Michael addition of β -keto esters, as their valine lithium enamides, as shown in Scheme 5.33 [174,175]. The lithium derivative adds directly to methylene malonic esters without further activation [174], but is not reactive enough to add to methyl vinyl ketone or ethyl acrylate unless trimethylsilyl chloride is also added [175]. Interestingly, the absolute configuration of the product changes when HMPA is added to the reaction mixture. The rationale for this observation is that in the absence of HMPA, the electrophile coordinates to the lithium, taking the position of L in the chelated structure shown in the inset, thus delivering the electrophile to the *Re* (rear) face. When the strongly coordinating HMPA is present, it occupies the 'L' position and blocks the *Re* face, thereby directing the electrophile to the *Si* face.



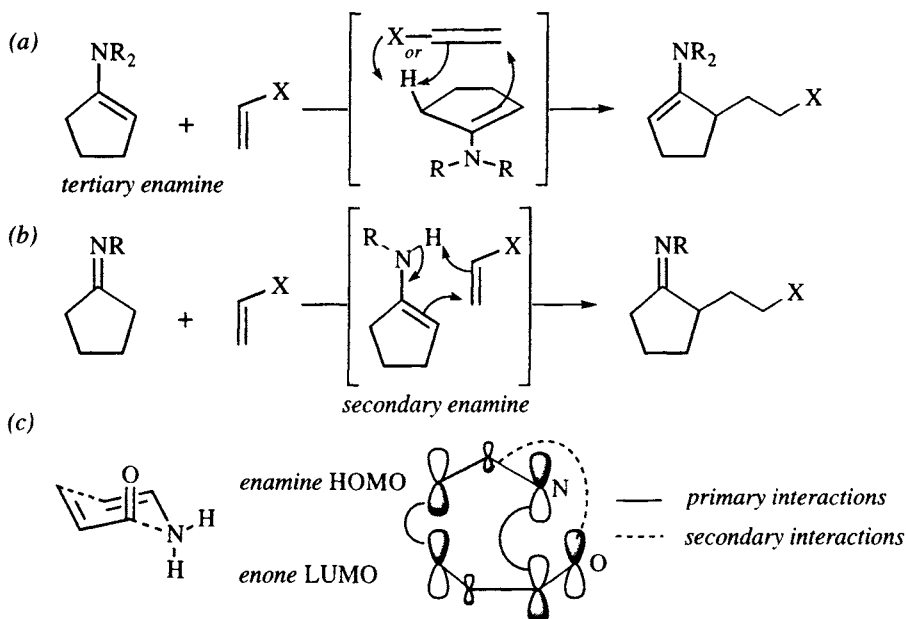
Scheme 5.33. Koga's asymmetric Michael additions of valine enamines of β -keto esters [174,175].

Enamines.¹⁷ The condensation of a secondary amine and a ketone to make an enamine is a well known reaction which has seen wide use in organic synthesis [176-178]. Imines of a primary amine and a ketone exist in a tautomeric equilibrium between the imine and secondary enamine forms, although in the absence of additional stabilization factors (*cf.* Scheme 5.33), the imine is usually the only detectable tautomer. Nevertheless, the enamine tautomer is very reactive toward electrophiles and Michael additions occur readily [179]. The mechanism of the Michael additions of tertiary and secondary enamines are shown in Scheme 5.34. For tertiary enamines, the Michael addition is accompanied by proton transfer from the α' -position to either the α -carbon or a heteroatom in the acceptor, affording the regioisomeric enamine as the initial adduct [180]. The proton transfer and the carbon-carbon bond forming operations may not be strictly concerted, but they are nearly so, since conducting the addition in deuterated methanol led to no deuterium incorporation [180].

With secondary enamines, there is also transfer of a proton, but this time from the nitrogen. Again, isotope labeling studies [181] suggest that the two steps are "more or less concerted" [179], in a reaction that resembles the ene reaction (Scheme 5.34b).

Theoretical studies indicate that these transition structures are probably influenced by frontier molecular orbitals (in addition to steric effects), as indicated in Scheme 5.34c [182]. For the reaction of aminoethylene (a primary enamine) and acrolein, the enamine HOMO and the enone LUMO have the most attractive interactions when aligned in the chair configuration shown, which has the enone in an *s-cis* conformation. Note that this orientation places the NH and the electrophile α -carbon in close proximity for proton transfer via the 'ene' transition structure.

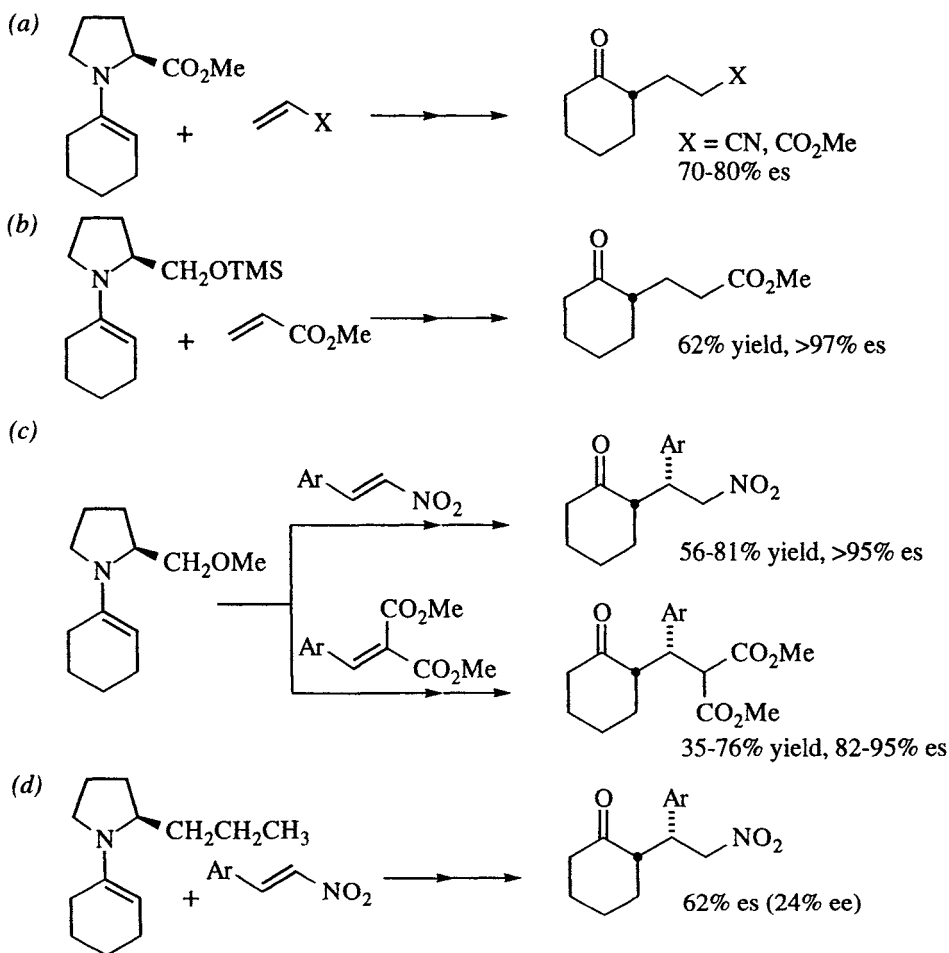
¹⁷ For a review of Michael additions of enamines, see ref. [149].



Scheme 5.34. (a) Suprafacial Michael addition-proton transfer of a tertiary enamine [180]. (b) aza-ene-like transition structure for secondary enamine Michael additions [179]. (c) Molecular orbital analysis of enamine and enone interactions [182].

Because the amines are removed in the subsequent hydrolytic workup, enamines are obviously amenable to an auxiliary-based asymmetric synthesis using a chiral amine. It is additionally significant from a preparative standpoint that unsymmetrical ketones alkylate at the less substituted position via tertiary enamines (*e.g.*, C₆ of 2-methylcyclohexanone) whereas the more hindered position is alkylated preferentially with secondary enamines (*e.g.*, C₂ of 2-methylcyclohexanone).

In 1969, Yamada demonstrated that the cyclohexanone enamine derived from proline methyl ester would add to acrylonitrile or methyl acrylate with 70-80% enantioselectivity (Scheme 5.35a, [183], but Ito later showed that the selectivity was much better if a prolinol ether was used instead (Scheme 5.35b, [184]. Seebach investigated the asymmetric Michael addition of enamines of prolinol methyl ether, as shown in the examples of Scheme 5.35c [195, 196], and likewise found outstanding

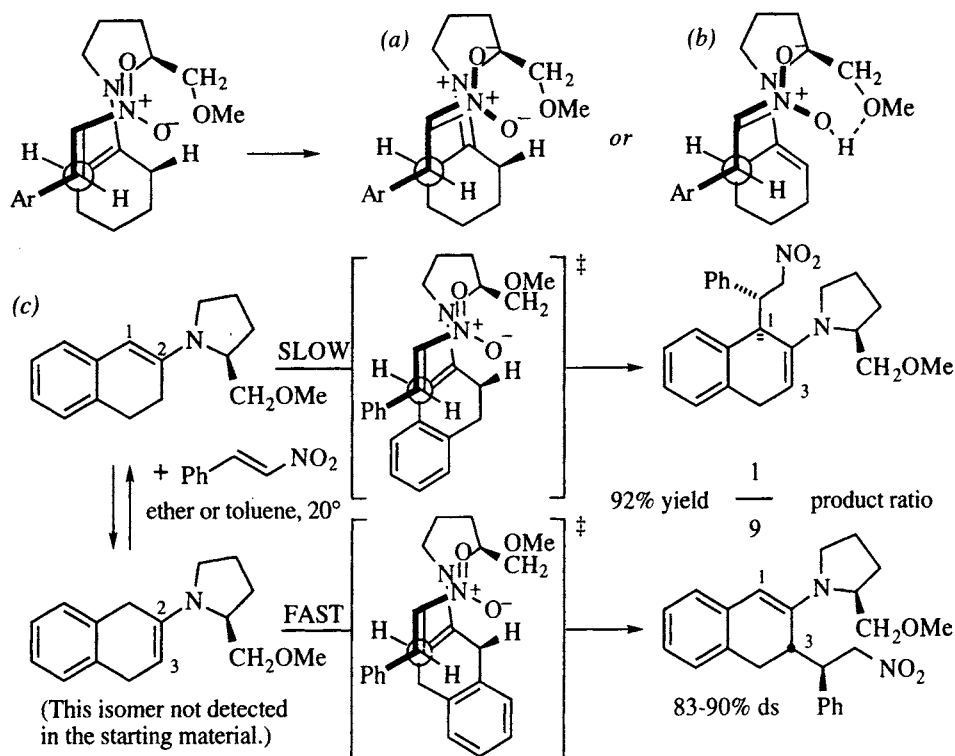


Scheme 5.35. Asymmetric Michael additions of chiral tertiary enamines. (a) [183]. (b) [184]. (c) [185], [186]. (d) [186].

the oxygen serves as a relay atom for a hydrogen transfer (another 'internal solvation' effect) such as illustrated in Scheme 5.36b (*cf.* Scheme 5.34a).

Other examples shed some light on the importance of the proton transfer in these enamine Michael additions. For example, the $\Delta^{1,2}$ enamine of β -tetralone (Scheme 5.36c) afforded high yields of 3-substituted $\Delta^{1,2}$ enamine products, even though the $\Delta^{2,3}$ enamine isomer was not present in the reaction mixture [187] (see also ref [188]). Under the reaction conditions (toluene or ether, stirring for 3-4 days), the $\Delta^{1,2}$ isomer must isomerize to the $\Delta^{2,3}$ isomer which reacts much faster, probably due to the greater acidity of the benzylic proton of the $\Delta^{2,3}$ isomer compared to the C_3 -proton of the $\Delta^{1,2}$ isomer.

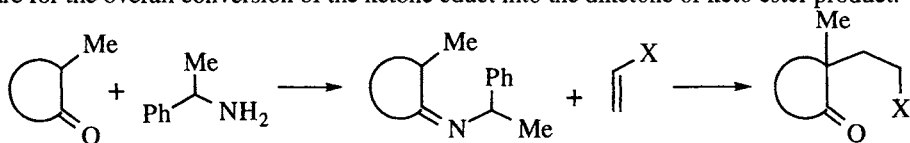
The asymmetric Michael addition of secondary enamines has been reviewed by d'Angelo [179]. Some of the more selective examples of this type of reaction are listed in Table 5.8. It is significant that these Michael additions are highly regio-selective, reacting virtually exclusively at the more highly substituted carbon, which affords α,α -disubstituted (quaternary) cyclopentanones, cyclohexanones, furans,



Scheme 5.36. Involvement of the methoxymethyl in the asymmetric Michael addition: (a) by dipolar stabilization of a zwitterion intermediate, or (b) by assisting in the proton transfer to the Michael acceptor. (c) Isolation of an addition product via enamine rearrangement [187].

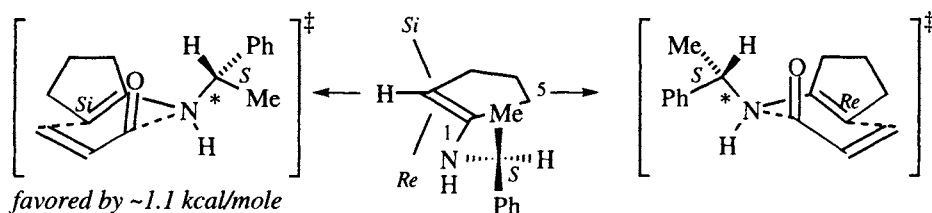
and pyrans in excellent yields and selectivities. An important advantage of this process is that it is stereoconvergent: racemic 2-substituted ketones are converted into nearly enantiopure products. Limitations are that a nitrogen in place of the oxygen of entries 7 and 8 is not possible, and that a carbomethoxy group decreases the enamine reactivity such that Lewis acid catalysis is required [179]. The mild conditions of these reactions (nonpolar solvents, room temperature) and the high overall yields make this an attractive process for large scale applications. The products of these reactions will catch the eye of anyone familiar with the Robinson annelation and related reactions [189,190], as these types of compounds are used as key building blocks in numerous natural product syntheses.

What is the origin of the regioselectivity, and what determines the face-selectivity of the Michael addition? The regioselectivity results from the aza-ene-like mechanism of this reaction. As shown in Scheme 5.37, although both enamines may form, reaction of the less substituted isomer is retarded by A^{1,3} strain effects. Note that in the aza-ene transition structure (Scheme 5.34b), the NH must be syn to the enamine double bond. Thus, the more highly substituted enamine isomer, in its most stable conformation, is in the proper conformation for Michael addition. In contrast, the reactive conformer of the less substituted isomer is destabilized by severe destabilizing steric interactions (A^{1,3} strain) between the ring substituent and the nitrogen substituent, which increase as the carbon-nitrogen bond gains double bond character in the transition state.

Table 5.8. Michael additions to cyclic ketones and lactones via their secondary enamines. The yields listed are for the overall conversion of the ketone educt into the diketone or keto ester product.

Entry	Ketone	Acceptor	Amine	Product	% Yield	% es	Ref.
1					n=1, 83	94	[191]
2					n=2, 88	95	[191]
3					n=1, 83	95	[192]
4					n=2, 80	94	[179]
5					n=1, —	—	[179]
6					n=2, 75	99	[193]

The origin of the face selectivity was revealed by MNDO calculations of the chair transition structures shown in Scheme 5.38, which differ only in the face of the enamine to which the enone is attached. By constraining the two reactants into parallel planes 3 Å apart and rotating around the indicated (*) bond of each structure, the conformations shown were found to be the lowest in energy [179]. The ground state conformation probably approximates the center structure, with the benzylic carbon-hydrogen bond synperiplanar to C₁ of the cyclopentene due to repulsion of the methyl and phenyl groups by C₅. In the transition structures, the benzylic carbon-hydrogen bond rotates 60° and becomes synclinal to C₁. Comparison of these structures indicated an energy difference of about 1.1 kcal/mole, which corresponds closely to the value expected based on the observed selectivity [179].



Scheme 5.38. Calculated low energy conformers for *Re* and *Si* attack of acrolein on cyclopentanone *S*-phenethyl enamine [179].

Allyl anions. The sulfur and phosphorous-stabilized allyl anions shown in Figure 5.10 have been examined by the Hua and Hanessian groups in asymmetric Michael additions to several enones. In these auxiliaries, the sulfur and the phosphorous are stereogenic, and the phosphorous additionally has chiral ligands. Some of the more selective examples of Michael additions using these ligands are listed in Table 5.9.

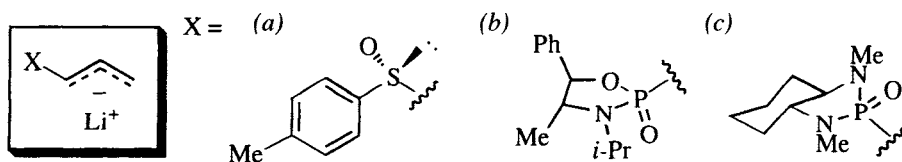


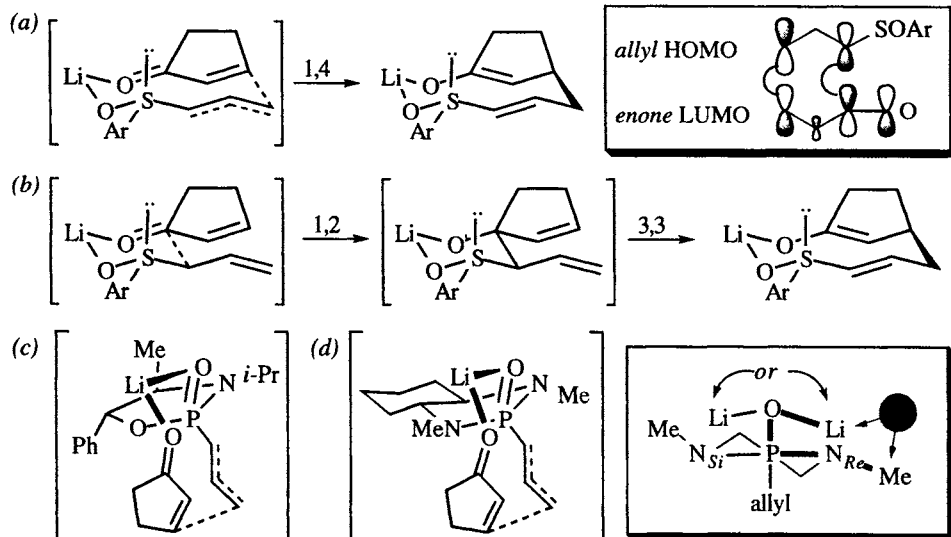
Figure 5.10. Auxiliaries for asymmetric Michael addition of allyl anions: (a) [195]. (b) [196]. (c) [197].

The mechanism of allylic sulfoxide addition is proposed to occur through a chelated 10-membered ring transition structure [198], as shown in Scheme 5.39a. The illustrated conformation features the favorable alignment of the molecular orbitals illustrated in the inset (*cf.* Scheme 5.34). However, it also has been suggested [148] that the reaction may proceed by sequential 1,2-addition followed by an alkoxide-accelerated Cope rearrangement,¹⁹ as shown in Scheme 5.39b. Note that the same conformation and orbital alignment are operative in this mechanism. For the addition of the phosphorous-stabilized allyllithium of Figure 5.10b and c, 10-membered rings are postulated [196,197]. The 10-membered rings shown in Schemes 5.39c and d have conformations similar to that shown in Scheme 5.39a; conceivably the tandem 1,2-carbonyl addition/3,3-Cope rearrangement suggested

¹⁹ Such a mechanism has been demonstrated in the addition of dithianyl allyl lithiums [199].

Table 5.9. Asymmetric Michael additions of sulfur and phosphorous stabilized allyllithiums. The X column refers to the auxiliaries in Figure 5.10.

		$\text{X}-\text{CH}_2\text{CH}=\text{CH}-\text{Li}^+$ + Michael acceptor \longrightarrow Product			
Entry	X	Acceptor	Product	% Yield	% es Ref.
1	a			n=1, 91	98 [195]
2	b			n=1, 79	99 [196]
3	c			n=1, 88	96 [197]
4	b			n=2, 70	94 [196]
5	b			n=3, 71	97 [196]
6	a			82	85 [195]
7	c			93	>99 [197]
8	a			80	97 [195]
9	c			75	97 [195]
10	c			80	96 [197]
11	c			76	>99 [197]

**Scheme 5.39.** Allyl sulfoxide additions; (a) 1,4-mechanism [198]. (b) Tandem 1,2-addition / 3,3-rearrangement mechanism [148] (see also ref. [199]). (c,d) Transition structures for allyl phosphine oxides [196,197]. *Inset:* Gauche pentane interaction between lithium and the N_{Re} methyl.

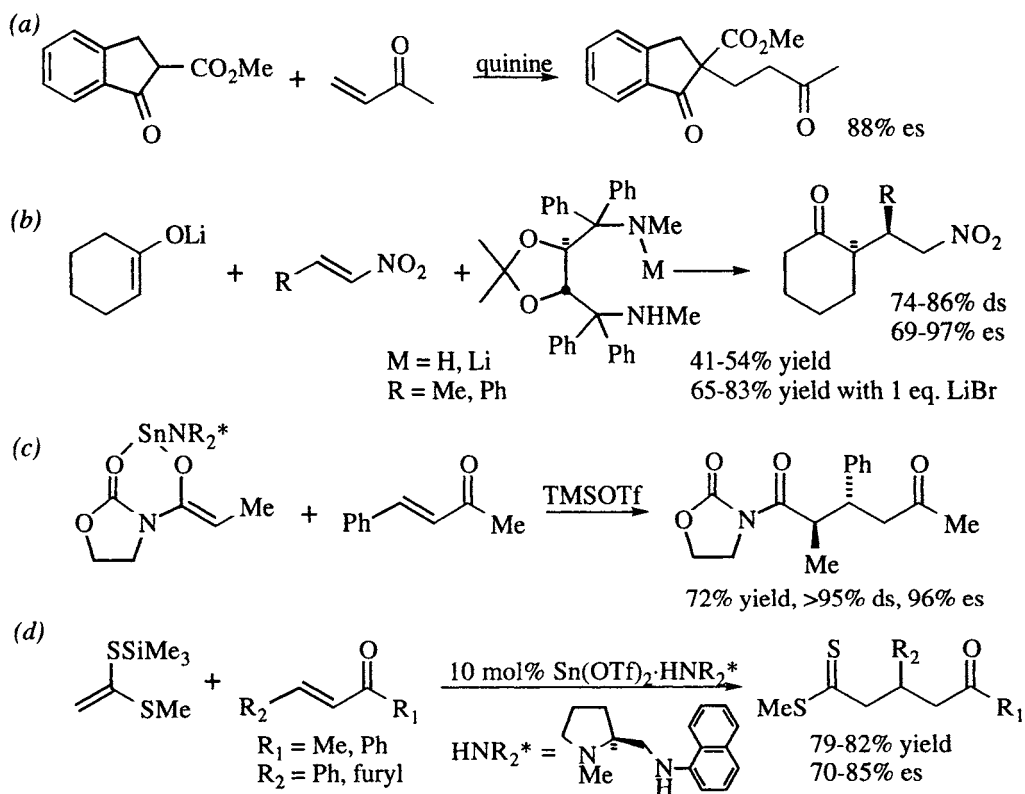
for the sulfoxides could intervene in these cases as well. For these auxiliaries, the site of lithium coordination to the phosphoryl group determines the chirality sense of the products. For the phosphaoxazolidine (Scheme 5.39c), the lithium coordinates anti to the bulky *N*-isopropyl substituent, but for the phosphaimidazolidine (Scheme 5.39d) the reason for the similar placement is not as obvious. The inset illustrates the 5-membered heterocycle in a half-chair conformation, with the *N*-methyls in pseudoequatorial configurations (the half chair is held rigid by the trans fused cyclohexane, which is deleted for clarity). The *N*-methyls are labeled according to their relative configurations on the stereogenic phosphorous. Note that coordination of the lithium syn to the *N*_{Re}-methyl generates a lithium/methyl interaction reminiscent of 2,3-*P*-3,4-*M* (gauche) pentane (cf. Figure 5.5). Coordination syn to the *N*_{Si}-methyl does not. Thus the latter site is preferred.

5.3.3 Interligand asymmetric induction

In considering Michael addition transition structures such as those generalized in Scheme 5.29, differentiation between two enantiomers of the same topicity can be achieved by introducing a stereogenic unit into either the donor (*vide supra*), the acceptor (*vide infra*) or the ligands on the metal. Metals can be efficiently complexed by crown ethers, and enolates form mixed aggregates with amines and lithium amides in solution. If an aggregate is chiral by virtue of a chiral ligand or a chiral crown, then interligand asymmetric induction can occur. As was true with the aldol addition (cf. Schemes 5.15-5.22), and enolate alkylations (cf. Schemes 3.23-3.26), chiral metal ligands offer the advantage of not requiring extra steps for the introduction and removal of an auxiliary, and may be amenable to catalysis. The examples illustrated below do not exhibit the outstanding selectivities that can be achieved by an auxiliary-based method, and there is little evidence upon which to base a rationale to explain the sense of asymmetric induction, but as knowledge of enolate/aggregate structures is gained, such insight will follow quickly and new systems with higher selectivities will undoubtedly emerge.

Following a 1973 lead by Långström and Bergson, who used a partially resolved amino alcohol as an asymmetric Michael catalyst [200], Wynberg used quinine as a catalyst for the asymmetric addition of 2-carbomethoxy-1-indanone to methyl vinyl ketone, obtaining 88% enantioselectivity in an optimized case (Scheme 5.40a), but the absolute configuration of the product was not determined [201]. Carbomethoxycyclohexanones could also be employed in this process, but the selectivities were low [201]. The Seebach group showed that cyclohexanone lithium enolates show good selectivities when complexed to chiral diamines or chiral lithium amides (Scheme 5.40b) [3]. They also noted significantly improved yields (and often improved selectivities) when an additional equivalent of lithium bromide was added to the recipe, results which clearly indicate the participation of enolate mixed aggregates in the reaction. The topicity (relative configuration of the stereocenters in the product) of this addition is consistent with a transition structure similar to that shown in Scheme 5.29c (see also Scheme 5.36). The Mukaiyama group explored the use of tin enolates complexed to chiral diamines as shown in Schemes 5.40c and d. The propionate imide enolate shown in Scheme 5.40c (when used in excess) adds to

benzal acetone with excellent selectivity [202]. The topicity of this addition is consistent with a mechanism similar to that shown in Scheme 5.29a, but note that titanium enolates of chiral imides added with low selectivity to β -substituted enones (Scheme 5.31d and e, [165]). If the dithioketene acetal shown in Scheme 5.40d is added slowly to a mixture of an enone, tin triflate, and chiral diamine, good enantioselectivities are achieved with catalytic amounts of tin and diamine [203]. The slow addition is necessary to keep a low concentration of the dithioketene acetal so as to minimize a competitive nonselective addition.



Scheme 5.40. (a) Wynberg's early example of interligand asymmetric induction in the Michael reaction [201]. (b) Seebach's investigation of cyclohexanone lithium enolate complexed to chiral diamines with extra lithium [3]. (c) Mukaiyama's imide tin enolate and chiral diamine [202]. (d) Mukaiyama's catalytic tin dithioenolate Michael addition [203].

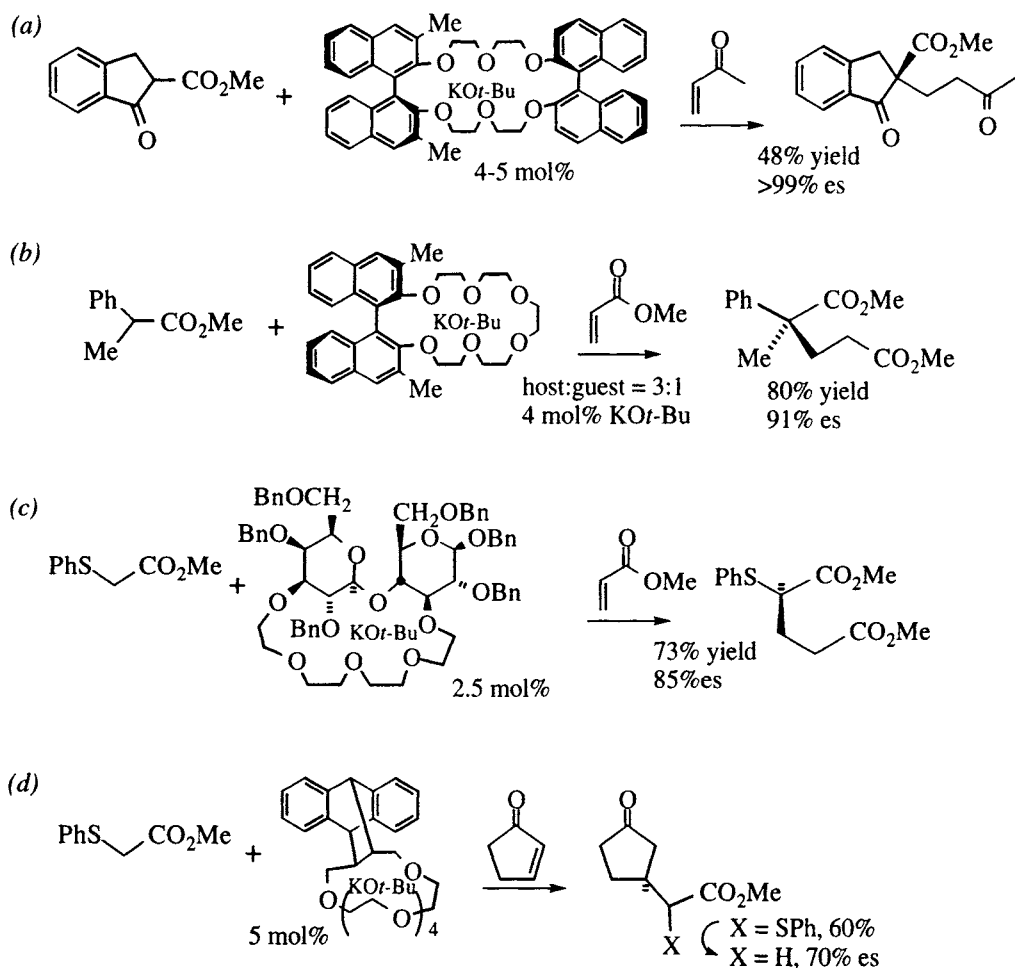
Complexation of potassium enolates with chiral crown ethers and Michael addition of the associated enolate has been investigated by several groups, illustrated by the examples shown in Scheme 5.41. For example, Cram used C₂-symmetric

acetate as nucleophile, and achieves reasonably high selectivities with small amounts of base and crown (Scheme 5.41c) [205]. Yamamoto added methyl thiophenyl acetate to cyclopentenone (Scheme 5.41d, [206]. The thiophenyl moiety of the addition product was reductively cleaved to afford a substituted cyclopentanone with a selectivity of 70% at the cyclopentanone β -carbon.

These four examples share the common feature of an acidic carbon stabilized by two functional groups, which permits employment of catalytic amounts of base and crown. The catalytic cycle is probably as follows [204]:

- 1) $\text{Crown} \cdot \text{K}^+ t\text{-BuO}^- + \text{H-R} \rightarrow \text{Crown} \cdot \text{K}^+ \text{R}^- + t\text{-BuOH}$
- 2) $\text{Crown} \cdot \text{K}^+ \text{R}^- + \text{C}=\text{C}-\text{C}=\text{O} \rightarrow \text{R}-\text{C}-\text{C}=\text{C}-\text{O}-\text{K}^+ \cdot \text{Crown}$
- 3) $\text{R}-\text{C}-\text{C}=\text{C}-\text{O}-\text{K}^+ \cdot \text{Crown} + \text{H-R} \rightarrow \text{R}-\text{C}-\text{CH}-\text{C}=\text{O} + \text{Crown} \cdot \text{K}^+ \text{R}^-$

The key step for catalyst turnover is the last one, whereby the enolate adduct deprotonates the next molecule of starting carbonyl. Clearly the initial carbon acid



Scheme 5.41. (a, b) Cram's C_2 -symmetric chiral crowns for asymmetric Michael addition [204]. (c) Penades's carbohydrate-based crown for asymmetric Michael additions [205]. (d) Yamamoto's chiral crown for asymmetric addition to β -substituted enones [206].

must be more acidic than the Michael product for this step to proceed. The two carbanion stabilizing groups in the above examples assure this fact, but also insure that epimerization in the product (if there are any α -protons left) can be a problem (cf. Scheme 5.41 c and d).

5.3.4 Chiral Michael acceptors

Posner has shown that enones having a chiral sulfoxide in the α -position are excellent receptors for conjugate addition of organometallics (Scheme 4.14, [207], and may also be used as Michael acceptors in enolate additions [208-210]. As with the addition of organometallics, the face selectivity can be rationalized based on either chelation of the metal by the enone and sulfoxide oxygens (Figure 5.11a) or by dipole alignment (Figure 5.11b) (cf. Scheme 4.16). In the following examples, which are chosen from others that are not as selective, the following trend emerges: enolates that are monosubstituted at the α -position follow the nonchelate (dipole) model, while α,α -disubstituted enolates follow the chelate model [211].

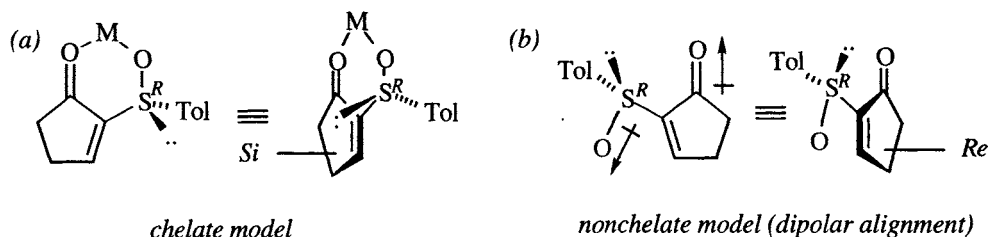
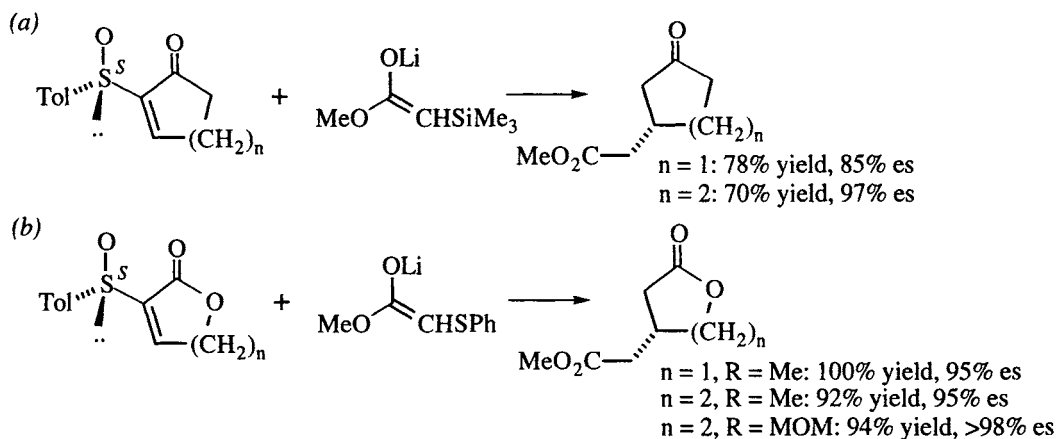


Figure 5.11. Models for face-selective addition of enolates to *R*-sulfoxides. (a) Chelate model predicts nucleophilic attack on *Si* face. (b) Nonchelate model, which has the C=O and S–O bonds antiperiplanar, predicts *Re* face attack.

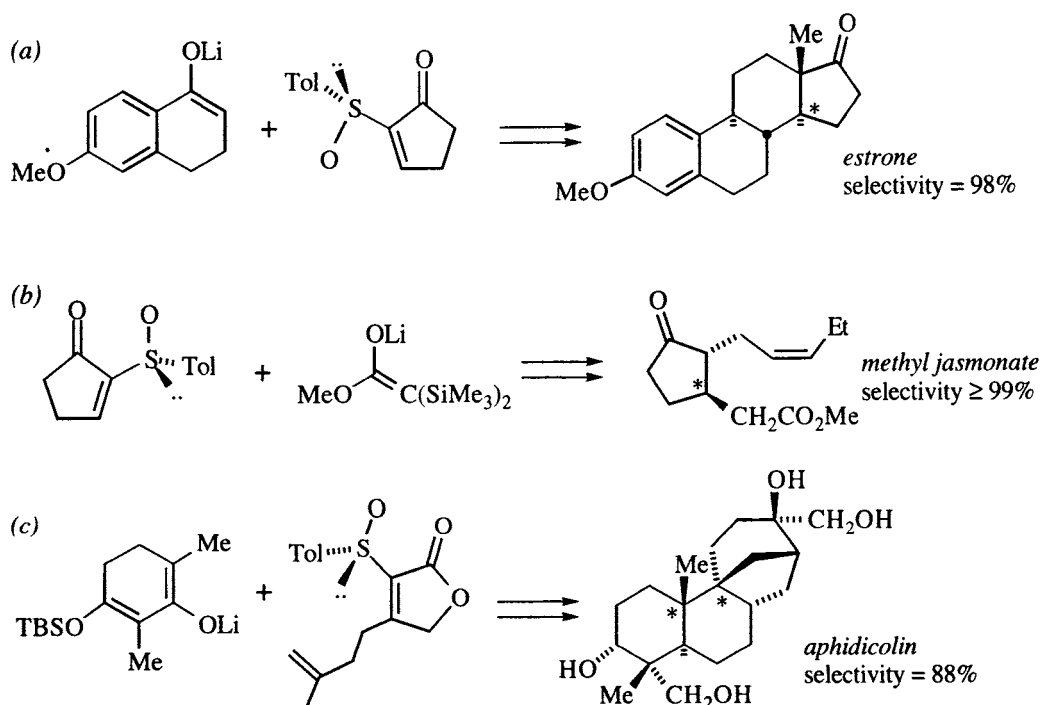
The lithium enolate of methyl trimethylsilyl acetate adds to cyclopentenone and cyclohexenone sulfoxides by the nonchelate model with good to excellent selectivity, as shown in Scheme 5.42a [210]. After the Michael addition, the sulfoxide and trimethylsilyl groups are removed, and the selectivity is assessed by determining the



Scheme 5.42. Sulfoxide mediated asymmetric Michael additions to (a) cycloalkenones and (b) lactones. Both are postulated to proceed via the nonchelate model, Figure 5.11b [210].

enantiomeric purity of the β -substituted ketone. Similarly, lithium enolates of phenylthioacetate esters add to five and six-membered lactones as shown in Scheme 5.42b [210]. The chirality sense of these products is consistent with a noncholate model: the nucleophile adds to the *Si* face of the *S* sulfoxide (*lk* topology).

Scheme 5.43 illustrates three applications of this methodology to total synthesis. The first example is taken from Posner's synthesis of estrone and estradiol [211], the second from Posner's synthesis of methyl jasmonate [212], and the third from Holton's synthesis of aphidicolin [213]. The latter is particularly noteworthy in that two contiguous quaternary centers are created in the asymmetric addition with excellent selectivity. In the estrone synthesis, the chirality sense of the product is consistent with the noncholate model, but the other two examples adhere to a chelate model. Note that the difference is the degree of substitution at the α -position of the enolate.



Scheme 5.43. Applications of sulfoxide Michael additions in natural product synthesis: (a) estrone [and estradiol] [211]. (b) methyl jasmonate [212]. (c) aphidicolin [213]. Stereocenters formed in the Michael addition are indicated (*).

5.4 References

1. H. E. Zimmerman; M. D. Traxler *J. Am. Chem. Soc.* **1957**, 79, 1920-1923.
2. D. Seebach *Angew. Chem. Int. Ed. Engl.* **1988**, 27, 1624-1654.
3. E. Juaristi; A. K. Beck; J. Hansen; T. Matt; T. Mukhopadhyay; M. Simson; D. Seebach *Synthesis* **1993**, 1271-1290.
4. P. G. Williard; Q.-Y. Liu *J. Am. Chem. Soc.* **1993**, 115, 3380-3381.

5. S. Masamune; S. A. Ali; D. L. Snitman; D. S. Garvey *Angew. Chem. Int. Ed. Engl.* **1980**, *19*, 557-558.
6. D. Seebach; V. Prelog *Angew. Chem. Int. Ed. Engl.* **1982**, *21*, 654-660.
7. R. W. Hoffmann *Angew. Chem. Int. Ed. Engl.* **1982**, *21*, 555-642.
8. W. R. Roush In *Comprehensive Organic Synthesis. Selectivity, Strategy, and Efficiency in Modern Organic Chemistry*; B. M. Trost, I. Fleming, Eds.; Pergamon: Oxford, 1991; Vol. 2, p 1-53.
9. I. Fleming In *Comprehensive Organic Synthesis. Selectivity, Strategy, and Efficiency in Modern Organic Chemistry*; B. M. Trost, I. Fleming, Eds.; Pergamon: Oxford, 1991; Vol. 2, p 563-593.
10. Y. Yamamoto; K. Maruyama *Heterocycles* **1982**, *18*, 357-386.
11. R. Hoffmann *Angew. Chem. Int. Ed. Engl.* **1982**, *21*, 555-566.
12. R. W. Hoffmann; G. Niel; A. Schlapbach *Pure Appl. Chem.* **1990**, *62*, 1993-1998.
13. H. C. Brown; P. V. Ramachandran *Pure Appl. Chem.* **1991**, *63*, 307-316.
14. Y. Yamamoto *Acc. Chem. Res.* **1987**, *20*, 243-249.
15. Y. Yamamoto; N. Asao *Chem. Rev.* **1993**, *93*, 2207-2293.
16. D. A. Evans In *Topics in Stereochemistry*; E. L. Eliel, N. L. Allinger, Eds.; Wiley-Interscience: New York, 1982; Vol. vol. 13, p 1-115.
17. R. W. Hoffmann; T. Herold *Chem. Ber.* **1981**, *114*, 375-383.
18. M. T. Reetz; T. Zierke *Chem. Ind. (London)* **1988**, 663-664.
19. W. R. Roush; A. E. Walts; L. K. Hoong *J. Am. Chem. Soc.* **1985**, *107*, 8186-8190.
20. E. J. Corey; C.-M. Yu; S. S. Kim *J. Am. Chem. Soc.* **1989**, *111*, 5495-5496.
21. U. S. Racherla; H. C. Brown *J. Org. Chem.* **1991**, *56*, 401-404.
22. H. C. Brown; U. S. Racherla; Y. Liao; V. V. Khanna *J. Org. Chem.* **1992**, *57*, 6608-6614.
23. U. S. Racherla; Y. Liao; H. C. Brown *J. Org. Chem.* **1992**, *57*, 6614-6617.
24. H. C. Brown; S. V. Kulkarni; U. S. Racherla *J. Org. Chem.* **1994**, *59*, 365-369.
25. R. P. Short; S. Masamune *J. Am. Chem. Soc.* **1989**, *111*, 1892-1894.
26. R. W. Hoffmann; H.-J. Zeiss *J. Org. Chem.* **1981**, *46*, 1309-1314.
27. H. C. Brown; K. S. Bhat *J. Am. Chem. Soc.* **1986**, *108*, 293-294.
28. H. C. Brown; P. K. Jadhav; K. S. Bhat *J. Am. Chem. Soc.* **1988**, *110*, 1535-1538.
29. A. G. M. Barrett; J. W. Malecha *J. Org. Chem.* **1991**, *56*, 5243-5245.
30. R. W. Hoffmann; A. Endesfelder; H.-J. Zeiss *Carbohydr. Res.* **1983**, *123*, 320-325.
31. W. R. Roush; L. K. Hoong; M. A. J. Palmer; J. C. Park *J. Org. Chem.* **1990**, *55*, 4109-4117.
32. W. R. Roush; R. L. Halterman *J. Am. Chem. Soc.* **1986**, *108*, 294-296.
33. W. R. Roush; L. K. Hoong; M. A. J. Palmer; J. A. Straub; A. D. Palkowitz *J. Org. Chem.* **1990**, *55*, 4117-4126.
34. J. Garcia; B. M. Kim; S. Masamune *J. Org. Chem.* **1987**, *52*, 4831-4832.
35. W. R. Roush; P. T. Grover; X. Lin *Tetrahedron Lett.* **1990**, *31*, 7563-7566.
36. W. R. Roush; P. T. Grover *Tetrahedron Lett.* **1990**, *31*, 7567-7570.
37. S. E. Denmark; E. J. Weber *Helv. Chim. Acta* **1983**, *66*, 1655-1660.
38. Y. Yamamoto; H. Yatagai; Y. Naruta; K. Maruyama *J. Am. Chem. Soc.* **1980**, *102*, 7107-7109.
39. S. E. Denmark; E. J. Weber *J. Am. Chem. Soc.* **1984**, *106*, 7970-7971.
40. K. Ishihara; M. Mouri; Q. Gao; T. Maruyama; K. Furuta; H. Yamamoto *J. Am. Chem. Soc.* **1993**, *115*, 11490-11495.
41. A. L. Costa; M. G. Piazza; E. Tagliavini; C. Trombini; A. Umani-Ronchi *J. Am. Chem. Soc.* **1993**, *115*, 7001-7002.
42. G. E. Keck; K. H. Tarbet; L. S. Geraci *J. Am. Chem. Soc.* **1993**, *115*, 8467-8468.
43. A. T. Nielsen; W. J. Houlihan *Org. React.* **1968**, *16*, 1-438.
44. C. H. Heathcock In *Comprehensive Organic Synthesis. Selectivity, Strategy, and Efficiency in Modern Organic Chemistry*; B. M. Trost, I. Fleming, Eds.; Pergamon: Oxford, 1991; Vol. 2, p 133-179.

45. T. Mukaiyama *Org. React.* **1982**, 28, 203-331.
46. S. Masamune; W. Choy; J. S. Petersen; L. R. Sita *Angew. Chem. Int. Ed. Engl.* **1985**, 24, 1-76.
47. C. H. Heathcock In *Comprehensive Carbanion Chemistry, Part B*; E. Buncl, T. Durst, Eds.; Elsevier: Amsterdam, 1984, p 177-237.
48. I. Paterson *Pure Appl. Chem.* **1992**, 64, 1821-1830.
49. C. H. Heathcock *Aldrichimica Acta* **1990**, 23, 99-111.
50. C. H. Heathcock In *Asymmetric Synthesis*; I. D. Morrison, Ed.; Academic: Orlando, 1984;

79. G. Helmchen; U. Leikauf; I. Taufer-Knöpfel *Angew. Chem. Int. Ed. Engl.* **1985**, *24*, 874-875.
80. W. Oppolzer; J. Blagg; I. Rodriguez; E. Walther *J. Am. Chem. Soc.* **1990**, *112*, 2767-2772.
81. W. Oppolzer; C. Starkemann; I. Rodriguez; G. Bernardinelli *Tetrahedron Lett.* **1991**, *32*, 61-64.
82. W. Oppolzer *Pure Appl. Chem.* **1988**, *60*, 39-48.
83. W. Oppolzer; C. Starkemann *Tetrahedron Lett.* **1992**, *33*, 2439-2442.
84. C. Siegel; E. R. Thornton *J. Am. Chem. Soc.* **1989**, *111*, 5722-5728.
85. A. Choudhury; E. R. Thornton *Tetrahedron Lett.* **1993**, *34*, 2221-2224.
86. J. R. Gage; D. A. Evans *Organic Syntheses* **1993**, *Coll. Vol. VIII*, 528-531.
87. D. A. Dickman; A. I. Meyers; G. A. Smith; R. E. Gawley *Organic Syntheses* **1990**, *Coll. Vol. VII*, 530-533.
88. M. Nerz-Stormes; E. R. Thornton *J. Org. Chem.* **1991**, *56*, 2489-2498.
89. T.-H. Yan; C.-W. Tan; H.-C. Lee; H.-C. Lo; T.-Y. Huang *J. Am. Chem. Soc.* **1993**, *115*, 2613-2621.
90. D. A. Evans; E. B. Sjogren; A. E. Weber; R. E. Conn *Tetrahedron Lett.* **1987**, *28*, 39-42.
91. L. N. Pridgen; A. F. Abdel-Magid; I. Lantos; S. Shilcrat; D. S. Eggleston *J. Org. Chem.* **1993**, *58*, 5107-5117.
92. S. Masamune; T. Sato; B. M. Kim; T. A. Wollmann *J. Am. Chem. Soc.* **1986**, *108*, 8279-8281.
93. I. Paterson; M. A. Lister; C. K. McClure *Tetrahedron Lett.* **1986**, *27*, 4787-4790.
94. A. I. Meyers; Y. Yamamoto *J. Am. Chem. Soc.* **1981**, *103*, 4278-4279.
95. A. I. Meyers; Y. Yamamoto *Tetrahedron* **1984**, *40*, 2309-2315.
96. I. Paterson; J. M. Goodman; M. A. Lister; R. C. Schumann; C. K. McClure; R. D. Norcross *Tetrahedron* **1990**, *46*, 4663-4684.
97. C. Gennari; C. T. Hewkin; F. Molinari; A. Bernardi; A. Comotti; J. M. Goodman; I. Paterson *J. Org. Chem.* **1992**, *57*, 5173-5177.
98. W. C. Still; D. Cai; D. Lee; P. Hauck; A. Bernardi; A. Romero *Lect. Heterocycl. Chem.* **1987**, *9*, 33-42.
99. E. J. Corey; R. Imwinkelreid; S. Pikul; Y. B. Xiang *J. Am. Chem. Soc.* **1989**, *111*, 5493-5495.
100. E. J. Corey; S. S. Kim *J. Am. Chem. Soc.* **1990**, *112*, 4976-4977.
101. E. J. Corey; C. P. Decicco; R. C. Newbold *Tetrahedron Lett.* **1991**, *32*, 5287-5290.
102. E. J. Corey; S. Choi *Tetrahedron Lett.* **1991**, *32*, 2857-2860.
103. E. J. Corey; D.-H. Lee; S. Choi *Tetrahedron Lett.* **1992**, *33*, 6735-6738.
104. E. J. Corey; D.-H. Lee *Tetrahedron Lett.* **1993**, *34*, 1737-1740.
105. R. O. Duthaler; P. Herold; W. Lottenbach; K. Oertle; M. Riediker *Angew. Chem. Int. Ed. Engl.* **1989**, *28*, 495-497.
106. R. O. Duthaler; P. Herold; S. Wyler-Helfer; M. Riediker *Helv. Chim. Acta* **1990**, *73*, 659-673.
107. T. Mukaiyama; T. Yura *Tetrahedron* **1989**, *45*, 1197-1207.
108. A. Ando; T. Shiori *Tetrahedron* **1989**, *45*, 4969-4988.
109. M. Muraoka; H. Kawasaki; K. Koga *Tetrahedron Lett.* **1988**, *29*, 337-338.
110. T. Mukaiyama; K. Banno; K. Narasaka *J. Am. Chem. Soc.* **1974**, *96*, 7503-7509.
111. K. Mikami; S. Matsukawa *J. Am. Chem. Soc.* **1993**, *115*, 7039-7044.
112. S.-i. Kiyooka; Y. Kaneko; M. Komura; H. Matsuo; M. Nakano *J. Org. Chem.* **1991**, *56*, 2276-2278.
113. S.-i. Kiyooka; Y. Kaneko; K.-i. Kume *Tetrahedron Lett.* **1992**, *33*, 4927-4930.
114. E. R. Parmee; O. Tempkin; S. Masamune; A. Abiko *J. Am. Chem. Soc.* **1991**, *113*, 9365-9366.
115. E. J. Corey; C. L. Cywin; T. D. Roper *Tetrahedron Lett.* **1992**, *33*, 6907-6910.
116. K. Furuta; T. Maruyama; H. Yamamoto *J. Am. Chem. Soc.* **1991**, *113*, 1041-1042.

117. K. Maruoka; H. Yamamoto In *Catalytic Asymmetric Synthesis*; I. Ojima, Ed.; VCH: New York, 1993, p 413-440.
118. S. Kobayashi; H. Uchiro; Y. Fujishita; I. Shiina; T. Mukaiyama *J. Am. Chem. Soc.* **1991**, *113*, 4247-4252.
119. S. Kobayashi; H. Uchiro; I. Shiina; T. Mukaiyama *Tetrahedron* **1993**, *49*, 1761-1772.
120. S. Kobayashi; M. Horibe *J. Am. Chem. Soc.* **1994**, *116*, 9805-9806.
121. S. Kobayashi; Y. Fujishita; T. Mukaiyama *Chem. Lett.* **1990**, 1455-1458.
122. T. Mukaiyama; S. Kobayashi; H. Uchiro; I. Shiina *Chem. Lett.* **1990**, 129-132.
123. W. R. Roush *J. Org. Chem.* **1991**, *56*, 4151-4157.
124. S. Masamune; M. Hirama; S. Mori; S. A. Ali; D. S. Garvey *J. Am. Chem. Soc.* **1981**, *103*, 1568-1571.
125. D. A. Evans; J. Bartroli *Tetrahedron Lett.* **1982**, *23*, 807-810.
126. I. Paterson; M. A. Lister *Tetrahedron Lett.* **1988**, *29*, 585-588.
127. S. Masamune In *Organic Synthesis: Today and Tomorrow*; B. M. Trost, C. R. Hutchinson, Eds.; Pergamon: Oxford, 1981, p 197-215.
128. S. F. Martin; W.-C. Lee *Tetrahedron Lett.* **1993**, *34*, 2711-2714.
129. S. F. Martin; G. J. Pacofsky; R. P. Gist; W.-C. Lee *J. Am. Chem. Soc.* **1989**, *111*, 7634-7636.
130. X. Chen; E. R. Hortelano; E. L. Eliel; S. V. Frye *J. Am. Chem. Soc.* **1992**, *114*, 1778-1784.
131. D. A. Evans; M. A. Calter *Tetrahedron Lett.* **1993**, *34*, 6871-6874.
132. D. A. Evans; J. L. Duffy; M. J. Dart *Tetrahedron Lett.* **1994**, *46*, 8537-8540.
133. D. A. Evans; M. J. Dart; J. L. Duffy; M. G. Yang; A. B. Livingston *J. Am. Chem. Soc.* **1995**, *117*, 6619-6620.
134. D. A. Evans; M. J. Dart; J. L. Duffy; D. L. Rieger *J. Am. Chem. Soc.* **1995**, *117*, 9073-9074.
135. I. Paterson; R. A. Ward; P. Romea; R. D. Norcross *J. Am. Chem. Soc.* **1994**, *116*, 3623-3624.
136. I. Paterson; R. D. N. A. Ward; P. Romea; M. A. Lister *J. Am. Chem. Soc.* **1994**, *116*, 11287-11314.
137. I. Paterson; J. M. Goodman; M. Isaka *Tetrahedron Lett.* **1989**, *30*, 7121-7124.
138. I. Paterson; R. D. Tillyer *J. Org. Chem.* **1993**, *58*, 4182-4184.
139. I. Paterson; C. K. McClure *Tetrahedron Lett.* **1987**, *28*, 1229-1232.
140. S. Masamune; P. A. McCarthy In *Macrolide Antibiotics. Chemistry, Biology, and Practice*; Academic: Orlando, 1984, p 127-198.
141. I. Paterson; M. M. Mansuri *Tetrahedron* **1985**, *41*, 3569-3642.
142. R. W. Hoffmann *Angew. Chem. Int. Ed. Engl.* **1987**, *26*, 489-594.
143. I. Paterson; M. V. Perkins *Tetrahedron Lett.* **1992**, *33*, 601-604.
144. D. A. Evans; R. L. Dow; T. L. Shih; J. M. Takacs; R. Zahler *J. Am. Chem. Soc.* **1990**, *112*, 5290-5313.
145. S. F. Martin; W.-C. Lee; G. J. Pacofsky; R. P. Gist; T. A. Mulhern *J. Am. Chem. Soc.* **1994**, *116*, 4674-4688.
146. I. Paterson; A. M. Lister; G. R. Ryan *Tetrahedron Lett.* **1991**, *32*, 1749-1752.
147. P. Perlmutter *Conjugate Addition Reactions in Organic Synthesis*; Pergamon: Oxford, 1992.
148. D. A. Oare; C. H. Heathcock In *Topics in Stereochemistry*; E. L. Eliel, N. L. Allinger, Eds.; Wiley-Interscience: New York, 1989; Vol. 19, p 87-170.
149. D. A. Oare; C. H. Heathcock In *Topics in Stereochemistry*; E. L. Eliel, N. L. Allinger, Eds.; Wiley-Interscience: New York, 1991; Vol. 20, p 227-407.
150. N. G. Rondan; M. N. Paddon-Row; P. Caramella; K. N. Houk *J. Am. Chem. Soc.* **1981**, *103*, 2436-2438.
151. K. N. Houk *Pure Appl. Chem.* **1983**, *55*, 277-282.
152. D. Seebach; J. Zimmerman; U. Gysel; R. Ziegler; T.-K. Ha *J. Am. Chem. Soc.* **1988**, *110*, 4763-4772.
153. T. Laube; J. D. Dunitz; D. Seebach *Helv. Chim. Acta* **1985**, *68*, 1373-1393.

154. H. B. Bürgi; J. D. Dunitz; E. Schefter *J. Am. Chem. Soc.* **1973**, *95*, 5065-5067.
155. N. T. Anh; O. Eisenstein *Nouv. J. Chimie* **1977**, *1*, 61-70.
156. H. B. Bürgi; D. Dunitz; J. M. Lehn; G. Wipff *Tetrahedron* **1974**, *30*, 1563-1572.
157. D. A. Oare; C. H. Heathcock *J. Org. Chem.* **1990**, *55*, 157-172.
158. D. A. Oare; M. A. Henderson; M. A. Sanner; C. H. Heathcock *J. Org. Chem.* **1990**, *55*, 132-157.
159. A. Bernardi; A. M. Capelli; A. Cassinari; A. Comotti; C. Genari; C. Scolastico *J. Org. Chem.* **1992**, *57*, 7029-7034.
160. W. Oppolzer; R. Pitteloud; G. Bernardinelli; K. Baettig *Tetrahedron Lett.* **1983**, *24*, 4975-4978.
161. E. J. Corey; R. T. Peterson *Tetrahedron Lett.* **1985**, *26*, 5025-5028.
162. G. Stork; N. A. Saccomano *Nouv. J. Chimie* **1986**, *10*, 677-679.
163. M. Yamaguchi; K. Hasebe; S. Tanaka; T. Minami *Tetrahedron Lett.* **1986**, *27*, 959-962.
164. D. A. Evans; F. Urpí; T. C. Somers; J. S. Clark; M. T. Bilodeau *J. Am. Chem. Soc.* **1990**, *112*, 8215-8216.
165. D. A. Evans; M. T. Bilodeau; T. C. Somers; J. Clardy; D. Cherry; Y. Kato *J. Org. Chem.* **1991**, *56*, 5750-5752.
166. D. A. Evans; J. M. Takacs *Tetrahedron Lett.* **1980**, *21*, 4233-4236.
167. P. E. Sonnet; R. R. Heath *J. Org. Chem.* **1980**, *45*, 3137-3139.
168. Y. Kawanami; Y. Ito; T. Kitagawa; Y. Taniguchi; T. Katsuki; M. Yamaguchi *Tetrahedron Lett.* **1984**, *25*, 857-860.
169. Y. Ito; T. Katsuki; M. Yamaguchi *Tetrahedron Lett.* **1984**, *25*, 6015-6016.
170. D. Enders; K. Papadopoulos *Tetrahedron Lett.* **1983**, *24*, 4967-4970.
171. D. Enders; K. Papadopoulos; B. E. M. Rendenbach *Tetrahedron Lett.* **1986**, *27*, 3491-3494.
172. D. Enders; B. E. M. Rendenbach *Chem. Ber.* **1987**, *120*, 1223-1227.
173. D. Enders; H. J. Scherer; J. Runsink *Chem. Ber.* **1993**, *126*, 1929-1944.
174. K. Tomioka; K. Ando; K. Yasuda; K. Koga *Tetrahedron Lett.* **1986**, *27*, 715-716.
175. K. Tomioka; W. Seo; K. Ando; K. Koga *Tetrahedron Lett.* **1987**, *28*, 6637-6640.
176. *Enamines: Synthesis, Structure, and Reactions*; 2nd ed.; A. G. Cook, Ed.; Marcel Dekker: New York, 1988.
177. *Enamines: Synthesis, Structure, and Reactions*; A. G. Cook, Ed.; Marcel Dekker: New York, 1969.
178. S. F. Dyke *The Chemistry of Enamines*; Cambridge: Cambridge, 1973.
179. J. d'Angelo; D. Desmaële; F. Dumas; A. Guingant *Tetrahedron Asymmetry* **1992**, *3*, 459-505.
180. U. K. Pandit; H. O. Huisman *Tetrahedron Lett.* **1967**, 3901-3905.
181. B. de Jeso; J.-C. Pommier *J. Chem. Soc., Chem. Commun.* **1977**, 565-566.
182. A. Sevin; J. Tortajada; M. Pfau *J. Org. Chem.* **1986**, *51*, 2671-2675.
183. S. Yamada; K. Hiroi; K. Achiwa *Tetrahedron Lett.* **1969**, 4233-4236.
184. Y. Ito; M. Sawamura; K. Kominami; T. Saegusa *Tetrahedron Lett.* **1985**, *26*, 5303-5306.
185. S. J. Blarer; W. B. Schweizer; D. Seebach *Helv. Chim. Acta* **1982**, *65*, 1637-1654.
186. S. J. Blarer; D. Seebach *Chem. Ber.* **1983**, *116*, 2250-2260.
187. S. Blarer; D. Seebach *Chem. Ber.* **1983**, *116*, 3086-3096.
188. G. Pitacco; F. P. Colonna; E. Valentin; A. Risalti *J. Chem. Soc., Perkin Trans. 1* **1974**, 1625-1627.
189. R. E. Gawley *Synthesis* **1976**, 777-794.
190. M. E. Jung *Tetrahedron* **1976**, *32*, 3-31.
191. M. Pfau; G. Revial; A. Guingant; J. d'Angelo *J. Am. Chem. Soc.* **1985**, *107*, 273-274.
192. J. d'Angelo; G. Revial; P. R. R. Costa; R. N. Castro; O. A. C. Antunes *Tetrahedron Asymmetry* **1991**, *2*, 199-202.
193. D. Desmaële; J. d'Angelo *Tetrahedron Lett.* **1989**, *30*, 345-348.
194. D. Desmaële; J. d'Angelo; C. Boix *Tetrahedron Asymmetry* **1990**, *1*, 750-760.

195. D. H. Hua; S. Venkataraman; M. J. Coulter; G. Sinai-Zingde *J. Org. Chem.* **1987**, 52, 719-728.
196. D. H. Hua; R. Chan-Yu-King; J. A. McKie; L. Myer *J. Am. Chem. Soc.* **1987**, 109, 5026-5029.
197. S. Hanessian; A. Gomtsyan; A. Payne; Y. Hervé; S. Beaudoin *J. Org. Chem.* **1993**, 58, 5032-5034.
198. M. R. Binns; O. L. Chai; R. K. Haynes; A. A. Katsifis; P. A. Shober; S. C. Vonwiller *Tetrahedron Lett.* **1985**, 26, 1569-1572.
199. F. E. Ziegler; U. R. Chakraborty; R. T. Webster *Tetrahedron Lett.* **1982**, 23, 3237-3240.
200. B. Långström; G. Berson *Acta Chem. Scand.* **1973**, 27, 3118-3119.
201. K. Hermann; H. Wynberg *J. Org. Chem.* **1979**, 44, 2238-2244.
202. T. Yura; N. Iwasawa; T. Mukaiyama *Chem. Lett.* **1988**, 1021-1024.
203. T. Yura; N. Iwasawa; K. Narasaka; T. Mukaiyama *Chem. Lett.* **1988**, 1025-1026.
204. D. J. Cram; G. D. Y. Sogah *J. Chem. Soc., Chem. Commun.* **1981**, 625-628.
205. M. Alonso-Lopez; J. Jimenez-Barbero; M. Martin-Lomas; S. Penades *Tetrahedron* **1988**, 44, 1535-1543.
206. M. Takasu; H. Wakabayashi; K. Furuta; H. Yamamoto *Tetrahedron Lett.* **1988**, 29, 6943-6946.
207. G. Posner In *Asymmetric Synthesis*; J. D. Morrison, Ed.; Academic: Orlando, 1983; Vol. 2, p 225-241.
208. G. Posner *Acc. Chem. Res.* **1987**, 20, 72-78.
209. G. H. Posner In *The Chemistry of Sulphones and Sulphoxides*; S. Patai, Z. Rapaport, C. Stirling, Eds.; Wiley: New York, 1988, p 823-849.
210. G. H. Posner; M. Weitzberg; T. G. Hamill; E. Asirvatham; H. Cun-heng; J. Clardy *Tetrahedron* **1986**, 42, 2919-2929.
211. G. H. Posner; C. Switzer *J. Am. Chem. Soc.* **1986**, 108, 1239-1244.
212. G. H. Posner; E. Asirvatham *J. Org. Chem.* **1985**, 50, 2589-2591.
213. R. A. Holton; R. M. Kennedy; H.-B. Kim; M. E. Krafft *J. Am. Chem. Soc.* **1987**, 109, 1597-1600.